Progress In Electromagnetics Research, PIER 9, 351–397, 1994

THEORETICAL STUDY OF ELECTROMAGNETIC PROPERTIESOF NON-LOCAL Ω MEDIA

M. M. I. Saadoun and N. Engheta

1. Introduction

Recently, we introduced the idea of a new class of electromagnetic materials, which we named pseudochiral Ω media [1–4, 7,8]. These materials, which fall into the category of bianisotropic media [5,6], can be conceptually thought of as a composite medium composed of an isotropic (or even anisotropic) host medium within which a large number of Ω–shaped metallic (or dielectric) microstructures can be embedded. These elements can be randomly located. However, they are to be all oriented in a given direction throughout the sample. For

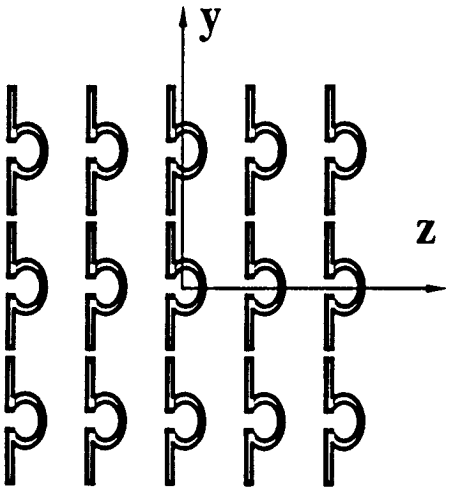

Figure 1. Bianisotropic local Ω medium composed of Ω microstructures lying in the $y-z$ plane, embedded in an isotropic host medium.

example, all the elements in the sample could be chosen to have the orientation shown in Fig. 1. For this orientation of Ω elements, the constitutive relations can be written as follows

$$\mathbf{D} = \underline{\underline{\varepsilon}} \cdot \mathbf{E} + \underline{\underline{\Omega}}_{em} \cdot \mathbf{B} \tag{1a}$$

$$\mathbf{H} = \underline{\underline{\mu}}^{-1} \cdot \mathbf{B} + \underline{\underline{\Omega}}_{me} \cdot \mathbf{E} \tag{1b}$$

where $\underline{\underline{\varepsilon}}$, $\underline{\underline{\mu}}$, $\underline{\underline{\Omega}}_{em}$, and $\underline{\underline{\Omega}}_{me}$ can have the following forms: $\underline{\underline{\varepsilon}} = \varepsilon_{xx}\hat{\mathbf{x}}\hat{\mathbf{x}} + \varepsilon_{yy}\hat{\mathbf{y}}\hat{\mathbf{y}} + \varepsilon_{zz}\hat{\mathbf{z}}\hat{\mathbf{z}}$, $\underline{\underline{\mu}} = \mu_{xx}\hat{\mathbf{x}}\hat{\mathbf{x}} + \mu_{yy}\hat{\mathbf{y}}\hat{\mathbf{y}} + \mu_{zz}\hat{\mathbf{z}}\hat{\mathbf{z}}$, $\underline{\underline{\Omega}}_{em} = -\mathrm{i}\Omega_c\hat{\mathbf{y}}\hat{\mathbf{x}}$, and $\underline{\underline{\Omega}}_{me} = -\mathrm{i}\Omega_c\hat{\mathbf{x}}\hat{\mathbf{y}}$. The parameter Ω_c is a measure of the coupling between electric and magnetic fields along the y and x axes, respectively. Among related problems on wave propagation in Ω media, one can mention the works reported in [1–4, 7, 8], and also the work on the use of approximate boundary conditions in [16], for treating electro-

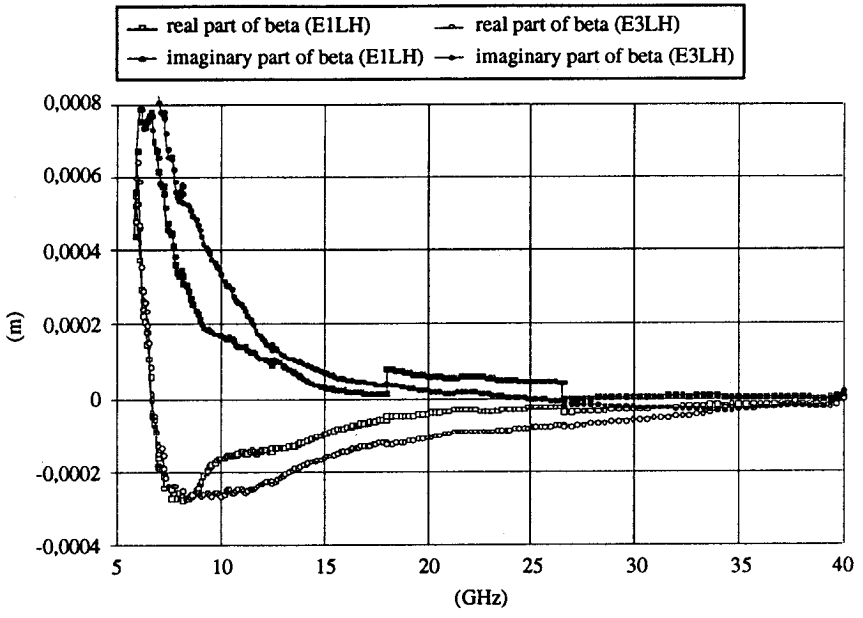

Figure 13. Real and imaginary parts of measured chirality parameter β for 1.7 vol.% three–turn left–handed helices in epoxy (E1LH), and 3.4 vol.% three–turn left–handed helices in epoxy (E3LH).

If the method of determination of the chirality parameter is fairly well adapted to our samples, it may not always be as satisfactory for the relative permittivity and the permeability. First of all, the equivalent homogeneous chiral medium approximation is probably more questionable. In addition, as mentioned in Section 2.5, inaccuracies in the S-parameters inversion due to thickness resonance phenomena unavoidably affect the results in certain frequency ranges. As a consequence, even though it is possible to compute ε and μ for a wide range of frequencies, the obtained values may not always be meaningful and can lead to erroneous conclusions regarding their dispersive behavior, which has a good probability to incorporate parasitic effects. Therefore, rather than presenting broadband data, we chose to give results for discrete frequencies. Values shown in Table 3 were obtained for EC3LH at five frequencies ranging from 18 to 38 GHz. They satisfy energy

loop parallel to the magnetic field H_z, in order for it to have maximum interaction with the electromagnetic field of the guided mode and hence, maximum effect on the stored electromagnetic energy density and consequently on the propagation constant. This can be done by having the omega (Ω) element presented in [1], which was the basis for the idea of single slab Ω phase–shifter.

By the geometry of its microstructures and their arrangements, the Ω medium is intended to strongly interact with the *guided* TE_{10} mode of a rectangular waveguide. This confined electromagnetic field has the property of having a longitudinal magnetic field component that is 90° out of phase with the transverse electric field. On the contrary, a *linearly polarized* uniform TEM plane wave propagating in an unbounded simple isotropic medium does *not* have this property. For such a wave, the electric and magnetic fields at any point are always *in phase* with each other. As the induced electric and magnetic dipoles of a conducting microstructure of the Ω type are always 90° out of phase with each other, it seems hopeless that one would be able to perturb the propagation constant of a linearly polarized TEM uniform plane wave using such conducting microstructures. Indeed our analysis of plane wave propagation through an unbounded Ω medium supports this fact that the wave number of a E_y–polarized plane wave propagating in the z direction is unaffected by the coupling parameter Ω_c [7].[1] We now introduce the following idea to overcome this problem.

2. Non-Local Ω Medium

If one considers the electric and magnetic fields of a linearly polarized TEM uniform plane wave at the same point in space, then they are found to oscillate in phase. But if one considers the same fields at two different points separated by a non-zero distance along the direction of the wave propagation, then, in general, the two sets of fields will not be completely in phase with respect to each other. For example, if the separation between the two points along the direction of propagation is equal to a quarter of a wavelength, then the electric field at any of

[1] Note that, although the Ω element does *not* affect the propagation constant of a uniform TEM plane wave, it *can* affect its wave impedance, i.e., the ratio of tranverse electric and magnetic fields [7].

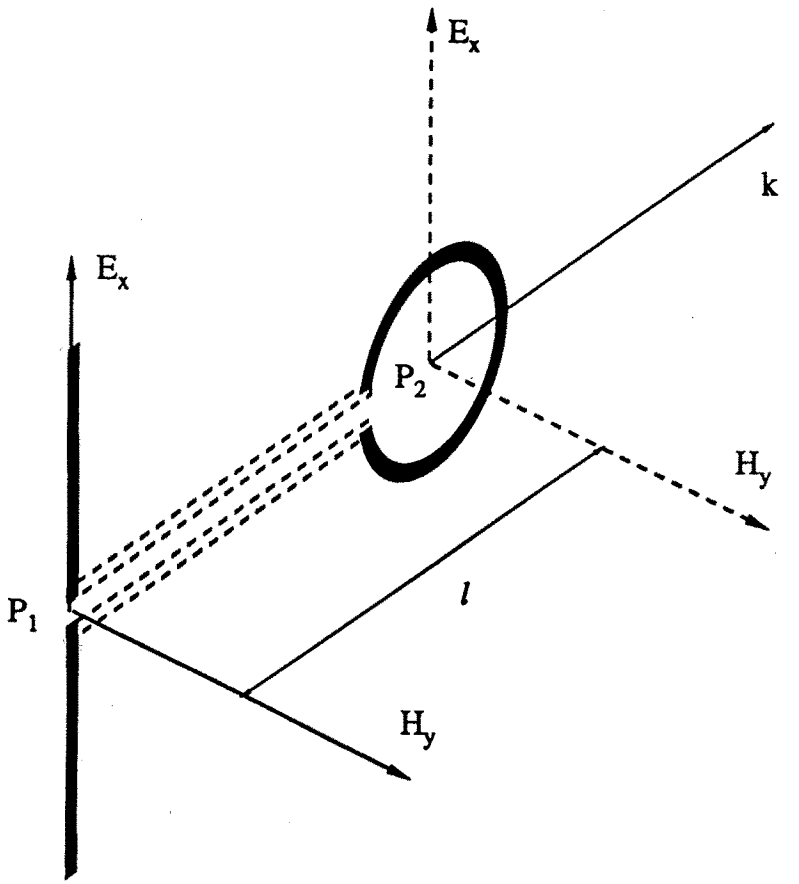

Figure 2. At any given point, point P_1 or P_2, the electric and magnetic fields of a TEM plane wave propagating in the z direction, are in phase with respect to each other. However, the fields at point P_1 can be out of phase with those at the point P_2, which lies a distance l ahead along the direction of wave propagation. If the stems of a conducting microstructure is aligned to interact with E_x at point P_1 and its loop to interact with H_y at P_2, and if the distance between the stems and loop does not affect the phase relationship between the induced electric and magnetic dipoles (as will be shown to be the case to within $\pm$, when the loop and stems are assumed to be small compared to the wavelength and the connecting transmission line is assumed lossless), then this structure can interact with the TEM wave.

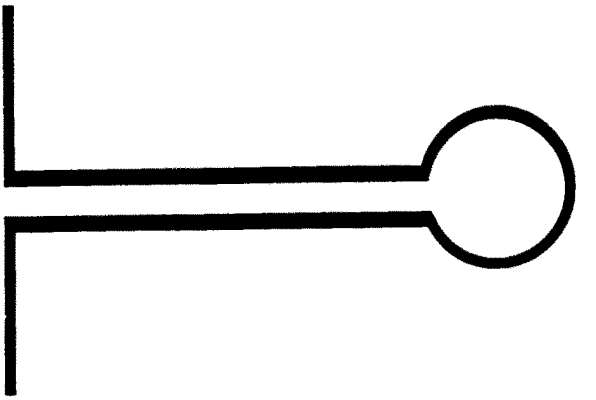

Figure 3. The non–local Ω element can be conceptually constructed by connecting the stems to the loop by means of a "tiny transmission line".

the two points is found to be 90° out of phase with the magnetic field at the other. Therefore, an electrically conducting microstructure, having its stems parallel to the electric field of a linearly polarized TEM wave at a given point and its loop axis parallel to the magnetic field at another point that is somewhat displaced from the first along the direction of the wave propagation, can, in principle, strongly interact with the field of the wave and hence perturb its wavenumber. Of course, this assertion implies the assumptions that the distance of the connection does *not* alter the phase relationship between the electric and magnetic dipoles and that the length of connection is *not* a multiple of half wavelength. These two issues will be addressed in more detail shortly. The orientation and relative positions of the stems and loop are illustrated in Fig. 2. Two questions that need to be answered are; (1) How can the two parts of the conducting microstructure be connected together?; and (2) Will this connection affect the phase relationship between the oscillating electric and magnetic dipoles? The physical connection between the stems and the loop can in principle be achieved by means of a "tiny transmission line" as shown in Fig. 3 [8]. We call the conducting element constructed in this way a *non–local Ω element,* since it couples the electric and magnetic fields at two points that are spatially

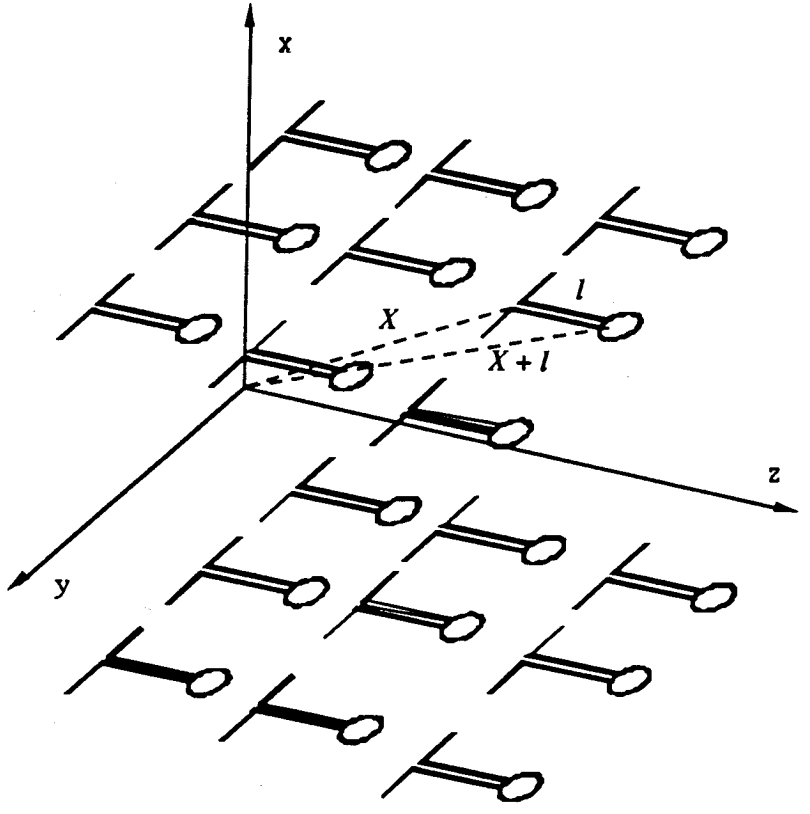

Figure 4. The non–local Ω medium can, in principle, be constructed by spreading a number of non–local Ω elements in an otherwise simple isotropic dielectric. The non–local Ω elements have to have a fixed orientation throughout the medium. However, to avoid periodicity of the medium, they can be placed at random positions relative to each other. Here $\mathcal{X}$ is the position vector of a general point in the medium, and $\boldsymbol{l}$ is the position vector of the loop center of any non–local Ω element in the medium, relative to the center of the air gap between the stems of the same element.

separated from each other, and since it reduces to the basic (local) Ω element introduced in our previous work [1–4], when the length of the connecting segment tends to zero. Furthermore, and for the sake of easy reference, we call the "tiny transmissions lines," connecting the stems of a non–local Ω element to its loop, an "Ω–transmission-line". If we consider a uniform TEM plane wave propagating along the direction of the Ω–transmission–line of the non–local Ω element, one can assume that the main interaction between the wave and the element takes place only at the positions of the stems and the loop. This is due to the fact that the Ω–transmission–line extends normal to the direction of the incident electric field. The interaction between the incident magnetic field and the Ω–transmission–line can also be neglected on the grounds that the separation between the two conductors of the Ω–transmission–line is very small and that the area covered by it is small compared to the (electrical) area of the loop. As for the second question, namely the effect of the length of the connection on the phase of the oscillating dipoles, it can be shown that, essentially no matter how long the connection is, the induced electric and magnetic dipoles still oscillate in phase quadrature with respect to each other.[2] The length of the connection can only affect the magnitude and sign of the coupling admittance Ω_c, but Ω_c remains basically a real function of frequency.[3] This fact follows from the properties of

[2] This is based on the assumption that the two dipoles at the two ends of this line are treated as reactive loads. A simple and direct way to demonstrate the validity of the above statement on the phase relation, is to point out that if a lossless transmission line is terminated by a reactive load at one end and a source at the other end, then the currents at its two ports can only differ in magnitude and sign, which means that their relative phase is either 0 or 180°. Since the charge accumulation on the stems has a 90° phase difference with the current flowing through them, it follows that the electric dipole at one end always has a $\pm 90°$ phase difference with the magnetic dipole at the other end.

[3] Strictly speaking, the material parameters of the medium cannot be purely real functions of frequency. This is due to the requirement imposed by the causality of the medium. The real and imaginary parts of material parameters of a causal medium should be related through Kramers–Kronig relations. In causal (ideally lossless) media with resonances that can be described by a Lorentzian model, the material

losslessness and reciprocity of the circuit model of the non–local Ω element, which are unaffected by the inclusion of a "transmission line" segment to the basic (local) Ω element. The *non–local pseudo–chiral Ω medium* itself can in principle be constructed by spreading a large number of the non–local Ω elements in an otherwise simple isotropic dielectric as shown in Fig. 4. Like in the case of the local Ω medium, the orientation of the elements has to be kept fixed throughout the medium although their relative locations can be random.

One reservation still needs to be addressed before we can write the constitutive relation of the non–local Ω medium. Usually when we talk about the constitutive relations of a medium, we implicitly assume that if scattering objects exist within the bulk of the medium, then they must be very small compared to the wavelength of the propagating field [9]. While this assumption is still applicable to the dimensions of the stems and the loop of the non–local Ω element, it may, in general, not be the case for the connection, i.e., Ω-transmission-line, between them. However, if we assume that the separation between the two wires of the transmission line in Fig. 3 is very small, then the interaction of the Ω–transmission–line with the *transverse* fields is very small as explained above. The transverse fields, therefore, only interact with the stems and the loop section of the non–local Ω elements, which are assumed to be small compared to wavelength. This allows us to express the medium interaction with the transverse fields in terms of constitutive relations, although these relations are, admittedly, expected to be more complex than those of a local Ω medium. The constitutive relations of the non–local Ω medium are themselves expected to take the form of non–local transformations relating the transverse fields $\mathbf{E}$ and $\mathbf{B}$ at a given point, to $\mathbf{D}$ and $\mathbf{H}$ at another. As for the longitudinal fields, i.e., the fields parallel to the Ω-transmission line, the only field component strongly affected by the Ω–transmission–line is the longitudinal electric field. For a TEM or a TE wave, this component vanishes anyway. For a TM wave, the effect of the Ω–transmission–line can be important. If the length of the Ω–transmission–line is small compared to the wavelength, this effect can be included in the longitudinal permittivity (i.e., ε_{zz} with z being the direction of propagation). Otherwise, the non–local Ω elements have to be treated as scattering objects of

---

parameters can be real for almost all real frequencies, while the imaginary part remains zero almost everywhere except at a set of frequencies (resonance frequencies) where it behaves like Dirac delta functions.

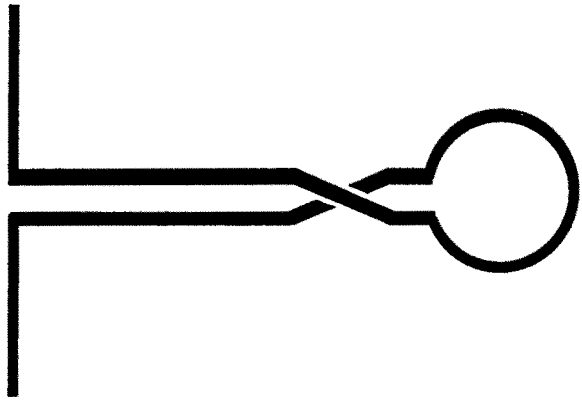

Figure 5. Twisting the loop by 180° around the axis of the Ω-transmission-line reverses the sign of Ω_c.

finite size. In the extreme case, where the density of the non–local Ω elements in the medium is high and where their length is also large compared to the wavelength, one may require the longitudinal electric field E_z to vanish in this medium as a result of the *effectively* "high longitudinal conductivity". That is, in this case the medium may not support TM modes.

3. Constitutive Relations of Non-Local Ω Media

With the restrictions mentioned at the end of the previous section in mind, the constitutive relations of the non–local Ω medium shown in Fig. 4 can be written as;

$$D_x(\mathbf{X}) = \varepsilon_{xx} E_x(\mathbf{X}) \tag{2a}$$

$$D_y(\mathbf{X}) = \varepsilon_{yy} E_y(\mathbf{X}) - \mathrm{i}\Omega_c B_x(\mathbf{X} + \boldsymbol{l}) \tag{2b}$$

$$D_z(\mathbf{X}) = \varepsilon_{zz} E_z(\mathbf{X}) \tag{2c}$$

$$H_x(\mathbf{X}) = \frac{1}{\mu_{xx}} B_x(\mathbf{X}) - \mathrm{i}\Omega_c E_y(\mathbf{X} - \boldsymbol{l}) \tag{2d}$$

$$H_y(\mathbf{X}) = \frac{1}{\mu_{yy}} B_y(\mathbf{X}) \tag{2e}$$

$$H_z(\mathbf{X}) = \frac{1}{\mu_{zz}} B_z(\mathbf{X}) \tag{2f}$$

where $\mathbf{X}$ is the position vector of a general point in the medium and $\boldsymbol{l}$ is the position vector of the loop center of any non-local Ω element in the medium relative to the center of the air gap between the stems of the same element. The coupling admittance dependence on the length l, as well as the frequency ω, is understood implicitly. The negative sign in front of $i\Omega_c$ is chosen for compatibility with Fig. 4. For the arrangement shown in that figure, and for a local medium, i.e., $l = 0$, the magnetic dipole moment pointing in the *negative* x-direction due to a typical Ω-element, *lags* 90° behind the electric dipole moment pointing in the *positive* y-direction due to the same element. Changing the sign of Ω_c of a non-local Ω-medium can, in principle, be achieved by twisting the loop 180° around the axis of the Ω-transmission-line, as shown in Fig. 5. For the Ω-element alignment shown in Fig. 3, and for the sign convention adopted in (2), the sign of Ω_c itself is *positive* (when $\boldsymbol{l} = 0$).

From (2), we notice that an unbounded non-local Ω medium possesses *translational* symmetry in the direction of the vector $\boldsymbol{l}$. We are going to refer to the direction of the vector $\boldsymbol{l}$ by the term "translational symmetry axis of the non-local Ω medium", or simply, the "symmetry axis" of the medium. As will be explained shortly, we shall assume that the non-local Ω medium always satisfies this symmetry requirement. The medium may or may not have other symmetry properties. For the most general non-local Ω medium, the symmetry axis can have an arbitrary direction with respect to the direction of the stems and the loop axes of the Ω elements. For simplicity, here we consider only the cases where the symmetry axis is normal to the stems and the loop axes. For example, in the case shown in Fig. 4, the loop axis is parallel to the x-axis, the stems are parallel to the y-axis, and the symmetry axis is parallel to the z-axis. For this particular medium, the constitutive relations can be written as;

$$D_x(x, y, z) = \varepsilon_{xx} E_x(x, y, z) \tag{3a}$$

$$D_y(x, y, z) = \varepsilon_{yy} E_y(x, y, z) - i\Omega_c B_x(x, y, z + l) \tag{3b}$$

$$D_z(x, y, z) = \varepsilon_{zz} E_z(x, y, z) \tag{3c}$$

$$H_x(x,y,z) = \frac{1}{\mu_{xx}} B_x(x,y,z) - \mathrm{i}\Omega_c E_y(x,y,z-l) \tag{3d}$$

$$H_y(x,y,z) = \frac{1}{\mu_{yy}} B_y(x,y,z) \tag{3e}$$

$$H_z(x,y,z) = \frac{1}{\mu_{zz}} B_z(x,y,z) \tag{3f}$$

Performing Fourier transformation with respect to the z-variable (the coordinate along the symmetry axis), we get for the electric field,

$$\mathbf{E}(x,y,z) = \frac{1}{\sqrt{2\pi}} \int_{-\infty}^{\infty} \tilde{\mathbf{E}}(x,y,k_z) \mathrm{e}^{\mathrm{i}k_z z}\, dk_z \tag{4}$$

and similar expressions for the fields **B**, **H** and **D**. Applying this transformation to both sides of (3), and equating the coefficients of the orthogonal $\mathrm{e}^{\mathrm{i}k_z z}$ functions on both sides we get,

$$\tilde{D}_x(x,y,k_z) = \varepsilon_{xx} \tilde{E}_x(x,y,k_z) \tag{5a}$$

$$\tilde{D}_y(x,y,k_z) = \varepsilon_{yy} \tilde{E}_y(x,y,k_z) - \mathrm{i}\Omega_c \mathrm{e}^{\mathrm{i}k_z l} \tilde{B}_x(x,y,k_z) \tag{5b}$$

$$\tilde{D}_z(x,y,k_z) = \varepsilon_{zz} \tilde{E}_z(x,y,k_z) \tag{5c}$$

$$\tilde{H}_x(x,y,k_z) = \frac{1}{\mu_{xx}} \tilde{B}_x(x,y,k_z) - \mathrm{i}\Omega_c \mathrm{e}^{-\mathrm{i}k_z l} \tilde{E}_y(x,y,k_z) \tag{5d}$$

$$\tilde{H}_y(x,y,k_z) = \frac{1}{\mu_{yy}} \tilde{B}_y(x,y,k_z) \tag{5e}$$

$$\tilde{H}_z(x,y,k_z) = \frac{1}{\mu_{zz}} \tilde{B}_z(x,y,k_z) \tag{5f}$$

It must be noted that the above equations are obtained assuming the uniformity of the medium in the direction of its translational symmetry axis. This assumption would make the medium parameters $\underline{\underline{\varepsilon}}$, $\underline{\underline{\mu}}$ and Ω_c to be independent of the z-coordinate. This property is required in order to be able to get simple Fourier-transformed constitutive relations, as given above. Equivalent to Fourier transform, one may simply assume that the field is propagating in the positive z-direction as $\mathbf{E}(x,y,z) = \tilde{\mathbf{E}}(x,y)\mathrm{e}^{\mathrm{i}k_z z}$. In this case, the constitutive relations take the form of those of a local medium since they reduce to,

$$D_x(x,y,z) = \varepsilon_{xx} E_x(x,y,z) \tag{6a}$$

$$D_y(x,y,z) = \varepsilon_{yy} E_y(x,y,z) - \mathrm{i}\Omega_c \mathrm{e}^{\mathrm{i}k_z l} B_x(x,y,z) \tag{6b}$$

$$D_z(x,y,z) = \varepsilon_{zz} E_z(x,y,z) \tag{6c}$$

$$H_x(x,y,z) = \frac{1}{\mu_{xx}} B_x(x,y,z) - \mathrm{i}\Omega_c \mathrm{e}^{-\mathrm{i}k_z l} E_y(x,y,z) \tag{6d}$$

$$H_y(x,y,z) = \frac{1}{\mu_{yy}} B_y(x,y,z) \tag{6e}$$

$$H_z(x,y,z) = \frac{1}{\mu_{zz}} B_z(x,y,z) \tag{6f}$$

where we have made the substitution, $B_x(x,y,z+l) = \tilde{B}_x(x,y)\,\mathrm{e}^{\mathrm{i}k_z(z+l)} = \mathrm{e}^{\mathrm{i}k_z l}\tilde{B}_x(x,y)\mathrm{e}^{\mathrm{i}k_z z} = \mathrm{e}^{\mathrm{i}k_z l} B_x(x,y,z)$ and similarly for $E_y(x,y,z-l)$. [4]

In the following section, we present the electric-field wave equation in the non–local Ω medium.

4. Electric-Field Wave Equation in Non-Local Ω Medium

The electric–field wave equation in the non–local Ω medium described by the set of constitutive relations given in (2) is found to

[4] The consititutive relations given in (5) or (6) have an interesting property; they are periodic in the *wavenumber* k_z. This is different from normal periodic structures where the medium parameters, and hence the constitutive relations, are periodic in the *space* variables. Here, the medium parameters are constant in space along the direction of propagation and, therefore, the medium does not constitute a spatially periodic structure in the usual sense. Some of the effects of periodicity in k_z are addressed in [7].

be,

$$\begin{aligned}
&\nabla \times \left\{ \underline{\underline{\mu}}^{-1} \cdot [\nabla \times \mathbf{E}(\mathbf{X})] \right\} - \omega^2 \underline{\underline{\varepsilon}} \cdot \mathbf{E}(\mathbf{X}) \\
&+ \omega \Omega_c \left\{ \left[\frac{\partial E_z(\mathbf{X}+\boldsymbol{l})}{\partial y} + \frac{\partial}{\partial z} [E_y(\mathbf{X}-\boldsymbol{l}) - E_y(\mathbf{X}+\boldsymbol{l})] \right] \hat{\mathbf{e}}_y \right. \\
&\left. - \frac{\partial E_y(\mathbf{X}-\boldsymbol{l})}{\partial y} \hat{\mathbf{e}}_z \right\} \\
&= \mathrm{i}\omega \mathbf{J}(\mathbf{X})
\end{aligned} \tag{7}$$

where $\mathbf{J}$ is the electric current density. This partial differential equation involves spatial derivatives of the electric field at different spatial points. The solution of this equation is clearly very difficult to obtain. If we assume that $\boldsymbol{l}$ extends parallel to the z-axis, and if we perform Fourier transform on this equation with respect to the z-coordinate, or alternatively, if we start from the Fourier transformed fields and constitutive relations as in (5), we get,

$$\begin{aligned}
&\nabla' \times \left\{ \underline{\underline{\mu}}^{-1} \cdot \left[\nabla' \times \tilde{\mathbf{E}}(\mathbf{X}_t, k_z) \right] \right\} - \omega^2 \underline{\underline{\varepsilon}} \cdot \tilde{\mathbf{E}}(\mathbf{X}_t, k_z) \\
&+ \omega \Omega_c \left\{ \left[\mathrm{e}^{\mathrm{i}k_z l} \frac{\partial \tilde{E}_z(\mathbf{X}_t, k_z)}{\partial y} + 2k_z \sin(k_z l) \tilde{E}_y(\mathbf{X}_t, k_z) \right] \hat{\mathbf{e}}_y \right. \\
&\left. - \mathrm{e}^{-\mathrm{i}k_z l} \frac{\partial \tilde{E}_y(\mathbf{X}_t, k_z)}{\partial y} \hat{\mathbf{e}}_z \right\} \\
&= \mathrm{i}\omega \tilde{\mathbf{J}}(\mathbf{X}_t, k_z)
\end{aligned} \tag{8}$$

where,

$$\begin{aligned}
\nabla' &= \nabla_t + \mathrm{i}k_z \hat{\mathbf{e}}_z \\
\nabla_t &= \frac{\partial}{\partial x} \hat{\mathbf{e}}_x + \frac{\partial}{\partial y} \hat{\mathbf{e}}_y \\
\mathbf{X}_t &= (x, y)
\end{aligned} \tag{9}$$

For a uniform plane wave where the field is of the form $\mathbf{E}(X) = \mathbf{E}_0 e^{i\mathbf{k}.\mathbf{X}}$, the wave equation simplifies further to,

$$\begin{aligned}&\mathbf{k} \times \left\{ \underline{\underline{\mu}}^{-1} \cdot [\mathbf{k} \times \mathbf{E}_0] \right\} + \omega^2 \underline{\underline{\varepsilon}} \cdot \mathbf{E}_0 \\ &- \omega \Omega_c \left\{ \left[ik_y e^{ik_z l} E_{oz} + 2k_z \sin(k_z l) E_{oy} \right] \hat{\mathbf{e}}_y - ik_y e^{-ik_z l} E_{oy} \hat{\mathbf{e}}_z \right\} \\ &= -i\omega \mathbf{J}_0\end{aligned} \tag{10}$$

If a uniform plane wave propagates in a source–free unbounded region along the z–direction, i.e., when $k_x = k_y = 0$ and $k_z = \beta$, with its electric field polarized along the y–axis, i.e., when $E_{ox} = E_{oz} = 0$, then we get,

$$\left[\omega^2 \mu_{xx} \varepsilon_{yy} - \beta^2 - 2\omega \mu_{xx} \Omega_c \beta \sin(\beta l) \right] E_{oy} = 0 \tag{11}$$

In this case, the propagation constant is a solution of the equation

$$\omega^2 \mu_{xx} \varepsilon_{yy} - \beta^2 - 2\omega \mu_{xx} \Omega_c \beta \sin(\beta l) = 0 \tag{12}$$

This shows that, in general, for such a TEM plane wave, the propagation constant depends to the first order on the coupling admittance of the medium Ω_c, as long as the length of the connecting section is different from zero, i.e. $l \neq 0$. Thus, the non–local Ω medium does indeed affect the propagation constant of a linearly polarized TEM uniform plane wave, as intuitively predicted earlier. For a very short connection, i.e., for $\beta l \ll 1$, and $\omega \mu_{xx} \Omega_c l \ll 1$, the solution of (12) is given, up to the first order in $\Omega_c l$, by,

$$\beta \approx \omega \sqrt{\mu_{xx} \varepsilon_{yy}} (1 - \omega \mu_{xx} \Omega_c l) \tag{13}$$

which confirms the first order dependence of the propagation constant on the coupling admittance. The complete study of eigenmodes of propagation of plane waves in an unbounded non–local Ω medium will be given shortly. But first in the next section, we will present a simplistic circuit model of the non–local Ω element that allows us to write approximate frequency-dependent expressions for the material parameters of the non–local Ω medium.

5. Circuit Model Analysis for Frequency Characteristics of Ω Media

The mere presence of a finite-length "transmission–line" segment as part of the non–local Ω element makes its frequency response non–trivial. In this section, we discuss an approximate circuit–model analysis for the frequency characteristics of electromagnetic wave scattering from non–local Ω elements. Before we start developing our model, we would like to mention from the beginning that this model, which is based on representing the different parts of a typical non–local Ω medium by equivalent *lumped* circuit elements, is by its very nature limited to low and medium frequency ranges. The extrapolation of the results of this model to very high frequencies can result in inadequate results. In particular, as will be shown, we have found that in the limit of infinitely high frequency, the permeability as predicted by the circuit model is different from that of free space as it should be [11]. This is due to the fact that we assume the dimensions of the Ω–element loops to be small compared to the wavelength and also assume that the magnetic field is uniform across it. This approximation holds only at low and intermediate frequencies. Therefore, when we mention in the text the term "high frequency permeability," we actually mean the "*extrapolated* high-frequency permeability" as predicted by this model. Moreover, in this model we assume that the density of Ω element is not high, and the single-scattering method is considered. We first discuss the circuit–model for local Ω media, wherein the length of Ω–transmission–line is assumed to be zero. Then we will present the results of our model for the non–local Ω media.

(a) *The Case of Local Ω Medium*

Consider first, a straight piece of a perfectly conducting rod whose dimensions are identical to those of the two stems of the local Ω element, (i.e., $l = 0$) when joined together to form an electric dipole, without a loop or an air gap in between. The incident electric field tangential to the surface of the conducting electric rod acts as a source of electromotive force (e.m.f.). The total e.m.f. on this rod due to the incident electric field is equal to $E_t d$, where E_t is the incident tangential electric field and d is the length of the rod. This e.m.f. causes equal and opposite electric charges $\pm Q_C$ to accumulate on the

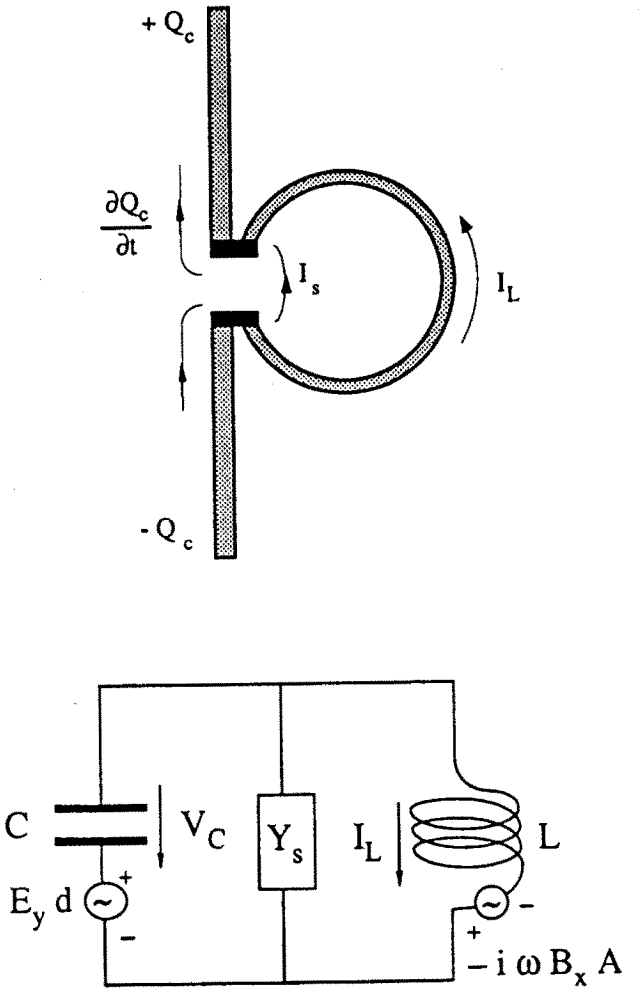

Figure 6. Part (a): The loop of the local Ω element interrupts the conduction current flowing at the center of the electric dipole. A fraction of this current goes to the stray capacitance associated with the air gap. Part (b): The equivalent circuit of the local Ω element consists of a capacitance, C, connected in series with an inductance, L. The stray capacitance associated with the air gap is represented by the shunt admittance Y_s. The equivalent circuit contains a voltage source in the capacitance branch, representing the tangential electric field and another in the inductance branch, representing the time–varying magnetic flux linkage.

opposite sides of the dipole. Since this e.m.f. is time varying, a current, equal to $\partial Q_C/\partial t$, flows along the dipole. It is well known that this process can be modeled as a voltage source of magnitude $E_t d$ in series with a capacitance C. Consider now that the conducting rod is divided into two parts with an air gap in between. In addition, consider that a loop made of a conducting material is connected across the air gap as shown in Fig. 6a. The connection is *local* in the sense that there is no "Ω–transmission line" connected in between. Therefore, the element constructed this way is the *local* Ω element. From the figure, it is clear that the loop interrupts the conduction current flowing at the center of the electric dipole. Therefore, the loop, represented by an inductance L, must be connected in series between the voltage source and the capacitor mentioned above. (The capacitance C of a short stem and the inductance L of a small loop can be expressed in terms of the stem's and loop's characteristics using quasi–static analysis, see e.g., [18]). Fig. 6a also shows that, due to the finite air gap between the two stems, part of the conduction current, originally flowing at the center of the dipole, does not enter the loop, but rather takes a shortcut through the stray capacitance associated with the air gap. Therefore, the equivalent circuit of the local Ω element can contain a stray admittance, representing the air gap, connected in parallel to the loop inductance. This equivalent circuit is shown in Fig. 6b, which also includes a second voltage source representing the e.m.f. induced in the loop by the time–varying magnetic flux linkage. For a local Ω element whose stems are aligned parallel to the y axis and whose loop's axis is pointed in the negative x direction, like the elements of the medium shown in Fig. 4, the equivalent–circuit voltage sources, i.e., e.m.f. due to tangential electric field and magnetic field are given, respectively, by;

$$e.m.f_{E_t} = E_y d \tag{14a}$$

$$e.m.f_{B_x} = -(-i\omega)(-B_x)A = -i\omega B_x A \tag{14b}$$

where A is the electrical cross–sectional area of the loop, and d is defined earlier. The approximation used in finding (14b) is valid only for low and intermediate frequencies where the wave length is large compared to the loop diameter and the magnetic field does not vary appreciably across the loop cross–section. As will be explained later, this same approximation is one of the reasons for the inadequacy of this approximate circuit model to correctly predict the very–high frequency

limit of the permeability of the medium. Another important point that needs clarification is the fact that, the magnetically-induced e.m.f. is due to the time variation of magnetic field *impressed* on the loop, i.e., the magnetic field produced by all sources *other than* the current induced in the loop by this impressed magnetic field. Therefore, (14b) can be replaced by $e_L = -i\omega\mu H_x A$ where μ is the permeability of the host dielectric in which the conducting microstructures are imbedded.

A simple analysis of the circuit in Fig. 6b shows that the capacitor voltage is given by

$$V_c = \frac{E_y d(1 - i\omega LY_s) - i\omega\mu H_x A}{1 - \omega^2 LC - i\omega LY_s} \tag{15a}$$

and the inductance current by,

$$I_L = \frac{-i\omega\mu H_x A(Y_s - i\omega C) - i\omega C E_y d}{1 - \omega^2 LC - i\omega LY_s} \tag{15b}$$

The electric charge accumulated on the edges of the stems is equal to the charge, Q_C, stored in the capacitor and is given by $Q_C = CV_C$. Since these equal and opposite charges are separated from each other by a distance d along the y axis, they constitute an electric dipole of moment $p_{yy} = Q_c d$. For an Ω medium containing N local Ω elements per unit volume, (when N is not high), the electric dipole moment per unit volume (polarization) along the y axis due to these elements is given (within the approximation used here) by

$$P_{yy} = Np_{yy} = \frac{NCd^2(1 - i\omega LY_s)E_y - i\omega CNAd\mu H_x}{1 - \omega^2 LC - i\omega LY_s} \tag{16}$$

From this equation, we find that the electrically-induced polarization is given by,

$$P_{e_{yy}} = \left\{ \frac{NCd^2(1 - i\omega LY_s)}{1 - \omega^2 LC - i\omega LY_s} \right\} E_y \tag{17a}$$

and that the magnetically-induced polarization is given by,

$$P_{m_{yy}} = \left\{ \frac{-i\omega CNAd}{1 - \omega^2 LC - i\omega LY_s} \right\} \mu H_x \tag{17b}$$

On the other hand, the current flowing in the loop produces a magnetic dipole moment which when measured in the *positive* x direction, is

given by $m_{xx} = -I_L A$. For a medium containing N elements per unit volume (with a similar assumption), the magnetic dipole moment per unit volume (magnetization) is given by,

$$M_{xx} = N m_{xx} = \frac{i\omega N\mu A^2(Y_s - i\omega C)H_x + i\omega CNAdE_y}{1 - \omega^2 LC - i\omega LY_s} \tag{18}$$

From this equation, we find that the magnetically–induced magnetization is given by,

$$M_{m_{xx}} = \left\{ \frac{i\omega N\mu A^2(Y_s - i\omega C)}{1 - \omega^2 LC - i\omega LY_s} \right\} H_x \tag{19a}$$

and that the electrically–induced magnetization is given by,

$$M_{e_{xx}} = \left\{ \frac{i\omega CNAd}{1 - \omega^2 LC - i\omega LY_s} \right\} E_y \tag{19b}$$

If the stray admittance Y_s is infinitely large, corresponding to an effective short circuit, then (17) and (18) reduce to,

$$P_{e_{yy}} = \left(NCd^2\right) E_y \qquad \text{and} \qquad P_{m_{yy}} = 0 \tag{20a}$$

$$M_{m_{xx}} = \left(\frac{-N\mu A^2}{L} \right) H_x \qquad \text{and} \qquad M_{e_{xx}} = 0 \tag{20b}$$

From these equations we see that the stray admittance has an important effect on the electrically–induced magnetization and the magnetically–induced polarization, and consequently on the coupling admittance Ω_c. In the above extreme example where the stray admittance is infinite corresponding to a short circuit, the Ω elements behave like disjoint conducting rods and loops with no coupling between them. In the other extreme where $Y_s = 0$, one can consider an ideal open–circuit gap at the junction between the stems and the loop. In this case, (17) and (19) have the form

$$P_{e_{yy}} = \left\{ \frac{NCd^2}{1 - \omega^2 LC} \right\} E_y \tag{21a}$$

$$P_{m_{yy}} = \left\{ \frac{-i\omega CNAd}{1 - \omega^2 LC} \right\} \mu H_x \tag{21b}$$

$$M_{m_{xx}} = \left\{ \frac{\omega^2 CN\mu A^2}{1 - \omega^2 LC} \right\} H_x \tag{21c}$$

$$M_{e_{xx}} = \left\{ \frac{i\omega CNAd}{1 - \omega^2 LC} \right\} E_y \tag{21d}$$

For convenience, the constitutive relations given by (2b) and (2d) are reproduced here for the case of a *local* Ω medium (i.e., $l = 0$) as $D_y = \varepsilon_{yy}E_y - \mathrm{i}\Omega_c B_x$ and $H_x = \frac{1}{\mu_{xx}}B_x - \mathrm{i}\Omega_c E_y$. Solving these equations for D_y and B_x, we get

$$D_y = \varepsilon_{yy_{\text{eff}}}E_y - \mathrm{i}\mu_{xx}\Omega_c H_x \tag{22a}$$

$$B_x = \mu_{xx}H_x + \mathrm{i}\mu_{xx}\Omega_c E_y \tag{22b}$$

where $\varepsilon_{yy_{\text{eff}}}$ is the effective permittivity in the y direction defined by,

$$\varepsilon_{yy_{\text{eff}}} = \varepsilon_{yy} + \mu_{xx}\Omega_c^2 \tag{23}$$

For the medium under consideration, we can write the displacement and magnetic induction vectors in the form, $\mathbf{D} = \varepsilon\mathbf{E} + \mathbf{P}_c$ and $\mathbf{B} = \mu(\mathbf{H} + \mathbf{M}_c)$, where the polarization and magnetization due to the host dielectric are included in the parameters ε and μ, while those due to the conducting Ω microstructures are incorporated in $\mathbf{P}_c$ and $\mathbf{M}_c$. Substituting for P_{yy} and M_{xx} from (21), we get,

$$D_y = \left\{\varepsilon + \frac{NCd^2}{1-\omega^2 LC}\right\}E_y - \mathrm{i}\mu\left\{\frac{\omega CNAd}{1-\omega^2 LC}\right\}H_x \tag{24a}$$

$$B_x = \left\{\mu + \frac{\omega^2 CN\mu^2 A^2}{1-\omega^2 LC}\right\}H_x + \mathrm{i}\mu\left\{\frac{\omega CNAd}{1-\omega^2 LC}\right\}E_y \tag{24b}$$

Comparison of (24) and (22) shows that the material parameters of the local Ω medium satisfy the following relations.

$$\varepsilon_{yy_{\text{eff}}} = \varepsilon + \frac{NCd^2}{1-\omega^2 LC} \tag{25a}$$

$$\mu_{xx} = \mu + \frac{\omega^2 CN\mu^2 A^2}{1-\omega^2 LC} \tag{25b}$$

$$\mu_{xx}\Omega_c = \mu\left\{\frac{\omega CNAd}{1-\omega^2 LC}\right\} \tag{25c}$$

The other material parameters not mentioned here, such as ε_{xx}, μ_{yy}, etc., are virtually unaffected by the presence of the conducting local Ω microstructures and are, therefore, equal to those of the host–dielectric material parameters ε and μ. Solving (25) for the parameters $\varepsilon_{yy}, \mu_{xx}$, and Ω_c, we get

$$\varepsilon_{yy} = \varepsilon \left\{ \frac{\left(1 + \frac{NCd^2}{\varepsilon}\right) - \left(1 - \frac{N\mu A^2}{L}\right)\omega^2 LC}{1 - \left(1 - \frac{N\mu A^2}{L}\right)\omega^2 LC} \right\} \tag{26a}$$

$$\mu_{xx} = \mu \left\{ \frac{1 - \left(1 - \frac{N\mu A^2}{L}\right)\omega^2 LC}{1 - \omega^2 LC} \right\} \tag{26b}$$

$$\Omega_c = \frac{\omega CNAd}{1 - \left(1 - \frac{N\mu A^2}{L}\right)\omega^2 LC} \tag{26c}$$

Unlike the parameter combinations appearing in (25), it is seen from (26), that if the parameters $\varepsilon_{yy}, \mu_{xx}$, and Ω_c are evaluated individually, the different medium parameters seem to have poles at *different* frequencies.[5] This is not a physically attractive feature, since the basic building block of the medium, viz. the local Ω element which is represented by an L–C circuit, has *one* natural resonance frequency. This natural resonance frequency should correspond to one simple pole in the medium parameters, which should be common to all physically meaningful expressions. Fortunately, the medium parameters do not appear alone by themselves in physically meaningful expressions. For example, as will be shown shortly, the medium's wave impedance for a y–polarized wave depends on the parameters $\varepsilon_{yy_{\text{eff}}}$ and μ_{xx}. Similarly, the wave equation for the same wave, given by (11), depends on the products $(\mu_{xx}\varepsilon_{yy})$ and $(\mu_{xx}\Omega_c)$. Here again, we can write the product $(\mu_{xx}\varepsilon_{yy})$ in terms of $(\mu_{xx}\varepsilon_{yy_{\text{eff}}})$ and $(\mu_{xx}\Omega_c)$. For this reason,

[5] If the density of the Ω elements is low, then the factor $(1 - N\mu A^2/L)$ is close to unity. In this case, the different material parameters will have poles at the same frequency $\omega = \frac{1}{\sqrt{LC}}$, and there will be approximately no distinction between ε_{yy} and ε_{eff}, and between μ and μ_{xx}.

for the remainder of this paper we use the set of material parameter combinations appearing in (25). Figure 7 shows plots of the set of material parameters given by (25) as function of frequency. This figure and (25) reveal several interesting properties of the local Ω–medium circuit-model described here. These features are;

(1) Assuming ε and μ of the host dielectric to be real, the medium is found to be *lossless* and *reciprocal*, since all parameters are real functions of frequency and $\Omega_{c_{em}} = \Omega_{c_{me}}$. [6] This follows directly from (24).

(2) If we set $L = 0$ and $A = 0$ in (25), corresponding to replacing the loop by a short circuit, we get the material parameters of a medium loaded with electric dipoles only, i.e.,

$$\varepsilon_{yy_{\text{eff}}} = \varepsilon \left(1 + \frac{NCd^2}{\varepsilon}\right) \tag{27a}$$

$$\mu_{xx} = \mu \tag{27b}$$

$$\mu_{xx}\Omega_c = 0 \tag{27c}$$

On the other hand, If we set $C = \infty$ and $d = 0$ in the same equations, corresponding to replacing the stems by a short circuit, we get the material parameters of a medium loaded with magnetic dipoles only, i.e.,

$$\varepsilon_{yy_{\text{eff}}} = \varepsilon \tag{28a}$$

$$\mu_{xx} = \mu \left(1 - \frac{N\mu A^2}{L}\right) \tag{28b}$$

$$\mu_{xx}\Omega_c = 0 \tag{28c}$$

Both sets of results can also be obtained by setting $Y_s = \infty$ in (17) and (19) and working out the steps leading to (25).

---

[6] The fact that the material parameters are real functions of frequency does not constitute a contradiction with causality because it can be shown that, in the limit of zero loss, the imaginary part of these material parameters tend to become Dirac–delta functions located at the resonance frequency. Therefore, strictly speaking, the imaginary parts do exist as Dirac–delta functions at resonance.

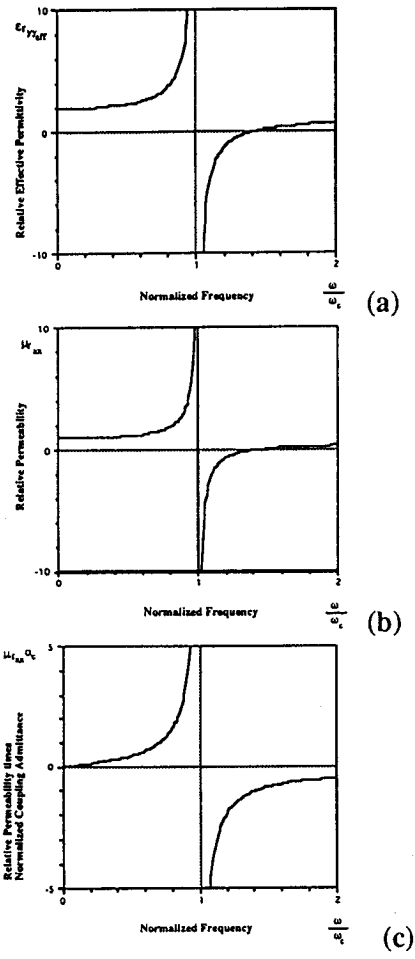

Figure 7. Parts (a), (b) and (c) show, respectively, the relative effective permittivity, the relative permeability, and the relative permeability times the normalized coupling admittance of a local Ω medium, plotted versus frequency. The frequency is normalized with respect to the natural resonance frequency of the Ω elements, i.e., $\omega_c = \frac{1}{\sqrt{LC}}$. For the plots presented here, we have assumed that the permittivity and permeability of the host dielectric are equal to free-space values, ε_o and μ_o, respectively. Here for the numerical values it is assumed that $NCd^2/\varepsilon = 1$ and $N\mu A^2/L = 1$. The fact that, for very high frequency limit, the extrapolated high frequency permeability differs from that of free space (μ_o) which is the physically expected value, is a consequence of approximating the Ω element by a *lumped-element* equivalent circuit. This point is further discussed in the text. It is also worth noting that the circuit–model analysis is limited to the low and intermediate frequency regimes. Nevertheless, here we plot the material parameters for wider range of frequency in order to see the behavior of this model in the higher frequency regime.

(3) At low frequencies, i.e., $\omega \ll \omega_c$, (25) simplify to,

$$\varepsilon_{yy_{\text{eff}}} = \varepsilon \left(1 + \frac{NCd^2}{\varepsilon}\right) \tag{29a}$$

$$\mu_{xx} = \mu \left[1 + \left(\frac{N\mu A^2}{L}\right)\left(\frac{\omega}{\omega_c}\right)^2\right] \tag{29b}$$

$$\mu_{xx}\Omega_c = \mu\omega CNAd \tag{29c}$$

Unlike the case of a medium containing separate conducting *closed* loops, whose permeability is described by (28b), the permeability of a local Ω medium is greater than the host's permeability (for low frequencies up to resonance frequency). Therefore, for this range of frequencies, local Ω media are effectively *paramagnetic* materials. This is due to the fact that here the loops of the Ω elements are open, being terminated by pairs of stems. Therefore, the frequency characteristics of the Ω microstructures are mainly determined by the capacitance between the stems at these low frequencies. Equation (29c) shows that at frequencies much lower than the resonance frequency, the coupling admittance Ω_c is proportional to the capacitance C and is independent of the inductance L. Therefore, increasing the capacitance C, without increasing the stray admittance Y_s, is a very important factor in improving the coupling admittance of the medium.

(4) At zero frequency, (25) reduce to,

$$\varepsilon_{yy_{\text{eff}}} = \varepsilon \left(1 + \frac{NCd^2}{\varepsilon}\right) \tag{30a}$$

$$\mu_{xx} = \mu \tag{30b}$$

$$\mu_{xx}\Omega_c = 0 \tag{30c}$$

while at very high frequencies, $\omega \to \infty$ they reduce to,

$$\varepsilon_{yy_{\text{eff}}} = \varepsilon \tag{31a}$$

$$\mu_{xx} = \mu \left(1 - \frac{N\mu A^2}{L}\right) \tag{31b}$$

$$\mu_{xx}\Omega_c = 0 \tag{31c}$$

From these equations, it is seen that at very high frequencies, the permittivity of the medium approaches that of the host dielectric, while

the permeability approaches the value predicted for a *diamagnetic* medium containing conducting closed loops only. These high frequency limits are evidently different from the permittivity and permeability of free space, ε_0 and μ_0. One reason for this discrepancy is the fact that we have ignored the frequency characteristics of the material parameters of the host dielectric itself. Including these characteristics removes the objection on the very–high–frequency limit of the medium permittivity, since ε of the host material itself tends to ε_0 at such frequencies. Resolving the problem of permeability requires μ of the host medium also to approach μ_0 for very high frequencies, and the second term in the parentheses in (31b) to vanish. One of the reasons that this term does not vanish in our model, is that we have assumed the e.m.f. induced in the loop to be proportional to the *product* of the magnetic induction B_x times the area of the loop A, rather than the *surface integral* of the former over the latter. This procedure implies the assumption that the loop is physically very small compared to the wavelength of the field, which obviously does not hold at infinitely high frequencies. Therefore, our model, though may be valid for frequencies beyond the resonance frequency of the conducting Ω elements, is *not* valid for *very high* frequencies. The high–frequency permeability of (31b) is obtained by extrapolating the results of our circuit model to infinitely high frequencies. Therefore, if we mention in the test the term "high-frequency permeability," we actually mean to say the "extrapolated high–frequency permeability". From (30) and (31), it is seen that the coupling admittance Ω_c vanishes at zero and infinite frequencies, in agreement with the symmetry properties and causality conditions known for coupling parameter of this kind such as chirality admittance [12,13].

(5) It is interesting to point out that, if the conducting local Ω elements are oriented *randomly* in the host dielectric, then the bulk coupling admittance Ω_c vanishes (in a statistical average sense) as expected, but the effects of the Ω elements on the bulk permittivity and permeability of the medium remain.

(b) *The Case of Non-Local Ω Medium*

The equivalent circuit of the non–local Ω element is obtained by including a finite–length section of a transmission line between the inductance and capacitance branches of the circuit of Fig. 6b. The resulting circuit is shown in Fig. 8, where we have omitted the shunt stray

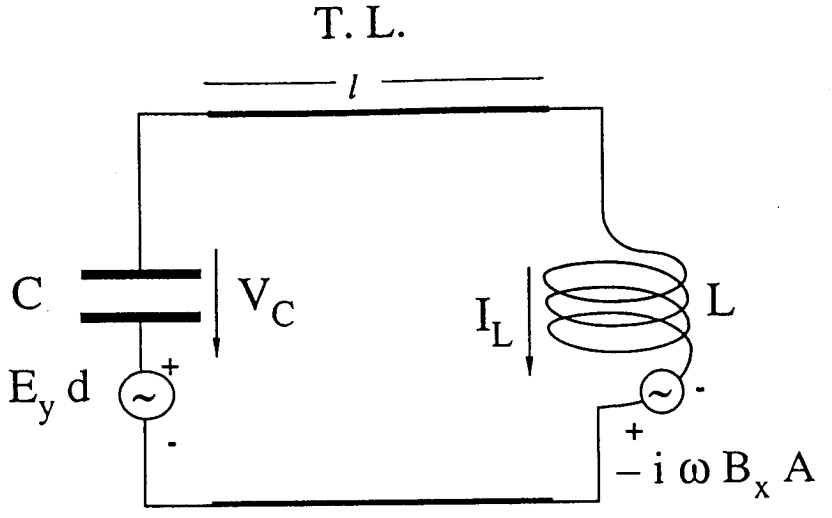

Figure 8. The equivalent circuit of the non–local Ω element. The shunt stray admittance at the entries to the transmission line is omitted for simplicity.

admittance at the two entry ports of the transmission line. Following the same line of analysis as for the case of the local Ω medium, we conclude that the non–local–Ω–medium material parameters affected by the presence of the Ω elements have the following forms;

$$\varepsilon_{yy_{\text{eff}}} = \varepsilon \left\{ 1 + \left(\frac{NCd^2}{\varepsilon} \right) \frac{\cos(k_d l) - \frac{\omega L}{Z_0} \sin(k_d l)}{(1 - \omega^2 LC)\cos(k_d l) - \frac{\omega L}{Z_0}\left[1 + Z_0^2 \left(\frac{C}{L}\right)\right] \sin(k_d l)} \right\} \quad (32a)$$

$$\mu_{xx} = \mu \left\{ 1 + \left(\frac{N\mu A^2}{L} \right) \frac{\omega^2 LC \cos(k_d l) + \frac{\omega L}{Z_0} \sin(k_d l)}{(1 - \omega^2 LC)\cos(k_d l) - \frac{\omega L}{Z_0}\left[1 + Z_0^2 \left(\frac{C}{L}\right)\right] \sin(k_d l)} \right\} \quad (32b)$$

$$\mu_{xx}\Omega_c = \mu \left\{ \frac{\omega CNAd}{(1 - \omega^2 LC)\cos(k_d l) - \frac{\omega L}{Z_0}\left[1 + Z_0^2 \left(\frac{C}{L}\right)\right] \sin(k_d l)} \right\} \quad (32c)$$

where Z_0 is the characteristic impedance of the "Ω-transmission line" and k_d the propagation constant of current and voltage signals along it. The propagation constant of local fields inside the Ω-transmission-line is *not* necessarily equal to the propagation constant of the *bulk* field propagating in the medium around the non-local Ω elements, even if they both propagate in the same direction. That is, in general, $k_d \neq k_z$. If we assume that the two wires of the tiny Ω-transmission-line are in the host medium, the value of k_d can be taken to be $k_d = \omega\sqrt{\mu\varepsilon}$ where ε and μ are the permittivity and permeability of the host medium. The basic difference between the non-local and local Ω medium is that, while in this circuit model the latter has a single resonance frequency corresponding to the natural resonance frequency of the L-C equivalent circuit of the local Ω element, the former has more than of one such resonance frequencies. This is due to the presence of the Ω-transmission line segment which works as a two port network that transforms the value of the impedance terminating one port, to a different value at the entrance to the other. For example, as seen from the

side of the Ω-transmission line attached to the stems, the impedance of the loop alternates between inductive and capacitive reactance as the operating frequency is increased. Similarly, as seen from the side of the Ω-transmission line attached to the loop, the impedance of the stems alternates between capacitive and inductive reactance. As a result, strictly speaking, the condition of resonance is satisfied many times as the operating frequency scans over all possible frequencies. It is worth noting that, for local Ω media, when the frequency is increased beyond the range of validity of lump circuit model, higher resonances can also be achieved. In this high frequency region, the stems and loops are no longer considered as small dipoles and small loops. The plots of the material parameter combinations appearing in (32) are shown in Fig. 9 for a typical non-local Ω element. Other than having multiple resonance frequencies, the effective permittivity and permeability have the simiar general characteristics as for a local medium. However, the product of permeability and coupling admittance changes sign each time a resonance frequency is crossed while it maintains the same sign between successive resonance frequencies.

In this section, using an approximate simplistic circuit model we have analyzed the material parameters of the non-local Ω medium. It is worth noting to reiterate that the circuit-model analysis presented here is limited to the low and intermediate frequency regimes. Nevertheless, here we studied this model for the wider range of frequency in order to see the behavior of this model in the higher frequency regime. In the next section we will present electromagnetic characteristics of plane wave propagation in the non-local Ω media.

6. Plane Wave Propagation in Unbounded Non-Local Ω Media

(a) *Propagation along the Medium's Translational Symmetry Axis*

The electric-field wave equation for the non-local Ω medium depicted in Fig. 4 was given earlier in Section IV for fields having different degrees of uniformity. For the most general case, the wave equation is given by (7). For an electric field that propagates along the translational symmetry axis of the medium and that has an arbitrary

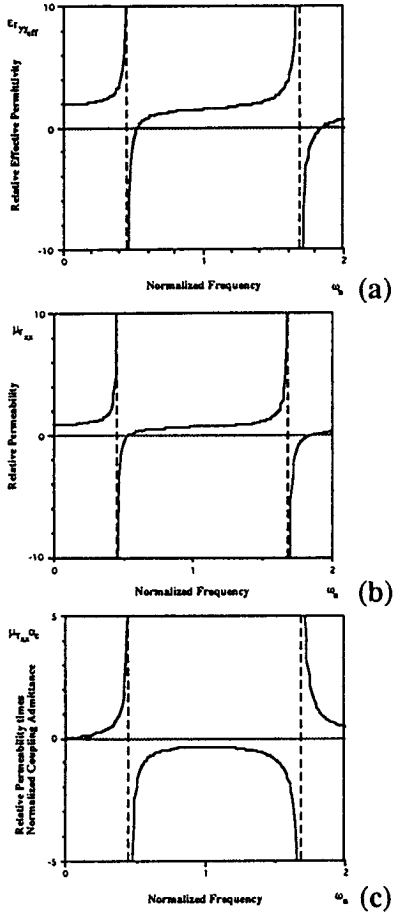

Figure 9. Parts (a), (b), and (c) show, respectively, the relative effective permittivity, the relative permeability, and the relative permeability times the normalized coupling admittance of a *non–local* Ω medium plotted versus frequency. These material parameters are calculated based on the lumped–element circuit model of the non–local Ω element. The frequency is normalized with respect to the natural frequency of the *local* Ω elements, i.e., $\omega_c = \frac{1}{\sqrt{LC}}$. The length of the transmission line connecting the loops and stems of the non–local Ω elements is chosen to equal to one quarter of the free–space wavelength of a uniform plane wave, whose frequency is equal to the natural resonance frequency, ω_c, of the local Ω elements. Other than that, the medium characteristics are the same as in Fig. 8. Note that the first resonance frequency occurs at a frequency substantially lower than the natural resonance frequency of the local Ω elements. Moreover, the medium has many resonance frequencies, two of which are shown in the figure. Note also that the sign of coupling admittance alternates between positive and negative as each resonance frequency is crossed. It is also worth noting that the circuit–model analysis is limited to the low and intermediate frequency regimes. Nevertheless, here we plot the material parameters for wider range of frequency in

transverse distribution, the wave equation is given by (8). For a uniform plane wave propagating in general direction, the wave equation is given by (10). For the special case of a y–polarized uniform plane wave propagating along the z axis of a source–free unbounded region, the wave equation is reduced to (11). In the last case, the wavenumber satisfies (12). Here, we solve (12) for a medium whose material parameters conform to our circuit model presented in section V. Then, in the next sub–section, we deal with the problem of uniform plane wave propagation in an arbitrary direction.

We first consider a local Ω medium, i.e., $l = 0$. In this case, (12) simplifies to,

$$\beta = k_0\sqrt{\mu_{r_{xx}}\varepsilon_{r_{yy}}} \equiv k_0\sqrt{\left[\mu_{r_{xx}}\varepsilon_{r_{yyeff}} - (\mu_{r_{xx}}\alpha_c)^2\right]} \tag{33}$$

where $k_0\left(=\omega\sqrt{\mu_0\varepsilon_0}\right)$ is the free-space wavenumber and $\alpha_c\left(\equiv \Omega_c\sqrt{\mu_0/\varepsilon_0}\right)$ is the normalized coupling admittance. Note that we have rearranged the right-hand side so that it contains only those material parameter combinations that appear in (25). Figure 10 shows a plot of the dispersion relation given by (33). The horizontal axis represents the free–space wavenumber normalized with respect to that of a uniform plane wave whose frequency is equal to the natural resonance frequency, $\omega_{co}\left(\equiv \frac{1}{\sqrt{LC}}\right)$, of the *local* Ω elements in vacuum. Since $k_0 \equiv \omega/c$ where c is the speed of light in vacuum, it follows that this axis also represents the normalized frequency. That is,

$$k_n \equiv \frac{k_0}{k_{co}} = \frac{\omega/c}{\omega_{co}/c} = \frac{\omega}{\omega_{co}} \equiv \omega_n \tag{34}$$

The vertical axis represents the medium's wavenumber normalized with respect to k_{co}. That is, $\beta_n \equiv \frac{\beta}{k_{co}}$. If we look back at the material parameters of the local Ω medium shown in Fig. 7, we see that in the frequency range $0 \leq \omega_n < 1$, the permittivity and permeability of the medium increase monotonically to infinitely large values at resonance $\omega_n = 1$. This explains the sharp increase in the propagation constant at resonance frequency. At very low frequencies, the permittivity of the medium increases due to the Ω elements while the permeability remains basically the same as that of the host dielectric. Therefore, the slope of the $\beta - k$ curve at low frequency is greater than

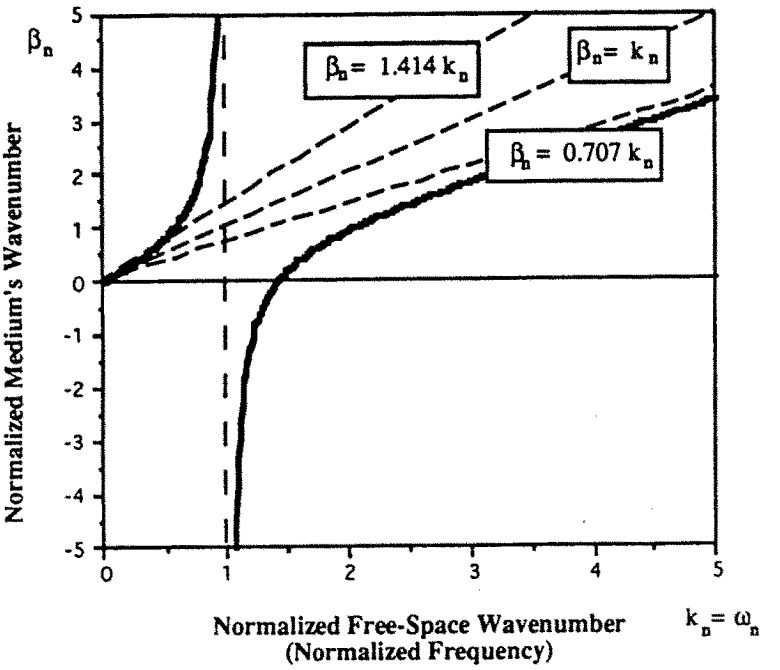

Figure 10. The normalized propagation constant of a *local* Ω medium plotted as function of normalized frequency. For simplicity, the material parameters of the host dielectric are taken equal to free-space values. The frequency is normalized with respect to the natural resonance frequency of the local Ω elements, i.e., $\omega_c = \frac{1}{\sqrt{LC}}$. Here for the numerical values it is assumed that $NCd^2/\varepsilon = 1$ and $N\mu A^2/L = 1$.

medium decreases while the permittivity approaches that of the host dielectric. Therefore, the slope of the $\beta - k$ curve at high frequency is less than unity. From the slope of the $\beta - k$ curve at high frequencies, we conclude that the local Ω elements can be used to reduce the propagation constant of a dielectric. This can be useful in slab waveguide applications. For example, if one can reduce the propagation constant of the host dielectric, by loading it with Ω elements, to a value lower than that of air (or free space), then one can prevent the slab waveguide

than that of air (or free space), then one can prevent the slab waveguide from supporting a surface-guided wave. However, the same, and even better, reduction in propagation constant can be obtained by simply loading the dielectric with electrically conducting *closed loops* without the need to attach stems to them. Constructed in this way, the medium becomes *diamagnetic* for all frequencies and its $\beta - k$ curve becomes identical to the lower asymptote in Fig. 10. Nevertheless, the reduction in wavenumber caused by the Ω elements has another distinct feature. Figure 10 shows that for frequencies slightly higher than the resonance frequency, the magnitude of the propagation constant drops to a very low value, and actually reaches zero for one specific frequency. This frequency lies at the boundary of the cutoff band, where the propagation constant becomes, in general, complex. For the choice of NCd^2/ε and $N\mu A^2/L$ used in calculating the graph of Fig. 10, the width of the cutoff band is zero. Figure 11 shows the normalized propagation constant of a local Ω medium having different values of NCd^2/ε and $N\mu A^2/L$. This medium has a finite cutoff band where the propagation constant becomes imaginary. This property can reduce the capability of slab waveguides to support guided-surface waves.

As far as wave propagation is concerned, the *non-local* Ω medium has two qualitative differences that distinguishes it from the *local* Ω medium. First, the medium exhibits multiple resonance frequencies for the circuit model presented here. Second, the propagation constant is different for positive and negative coupling admittance. The second feature actually constitutes the motivation for the conception of the non-local Ω medium. The propagation constant of this medium is governed by (12) which can be written in the form,

$$\omega^2 \left[\mu_{xx}\varepsilon_{y\text{eff}} - (\mu_{xx}\Omega_c)^2\right] - \beta^2 - 2\omega\,(\mu_{xx}\Omega_c)\,\beta\sin(\beta l) = 0. \qquad (35)$$

Figures 12 show the magnitude (with no sign accounted) of the normalized wavenumbers versus normalized frequency in two non-local Ω media, differing only in the sign of the coupling admittance. The media specifications are identical to those of the local Ω medium, whose dispersion diagram is plotted in Fig. 10, except that the length of the transmission lines connecting the loops to stems of the non-local Ω elements, is chosen to equal to one quarter of a free-space-wavelength at the resonance frequency of the local Ω elements, i.e., $l = 0.25\lambda_{co}$. (Remarks: These plots were actually calculated numerically assuming very small loss tangent of the host dielectric ($\delta = 10^{-6}$). Including

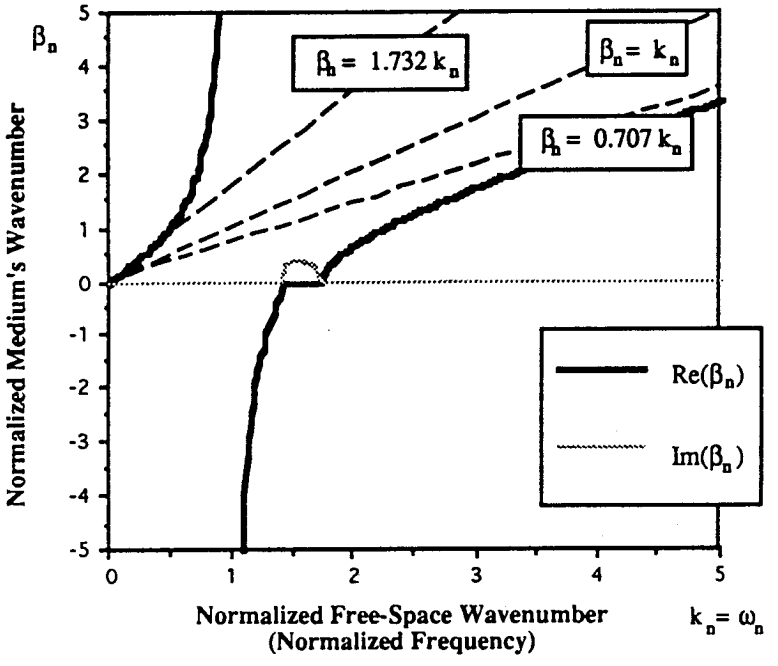

Figure 11. The same as in Fig. 10., except that $NCd^2/\epsilon = 2$ and $N\mu A^2/L = 1$. At low frequencies, the curve is tangential to the asymptote $\beta_n = \sqrt{3}k_n$, while at high frequencies, it converges to the asymptote $\beta_n = \sqrt{0.5}k_n$. This medium has a cutoff region of non–zero bandwidth.

the numerical solution of (35) by Newton's method. The curves shown are, therefore, the absolute value of the real part of the propagation constant. We made sure that the imaginary part corresponding to these curves (which is very small of the order 10^{-7}) is positive for all frequencies. It must also be mentioned that the numerical accuracy near resonance is much lower than that at a frequency far from it). Note that the propagation constants differ appreciably for the two media for frequencies beyond the first resonance frequency. Before we explain this difference, let us first discuss each diagram separately. If we look at the graphs of effective permittivity and permeability of a non–local

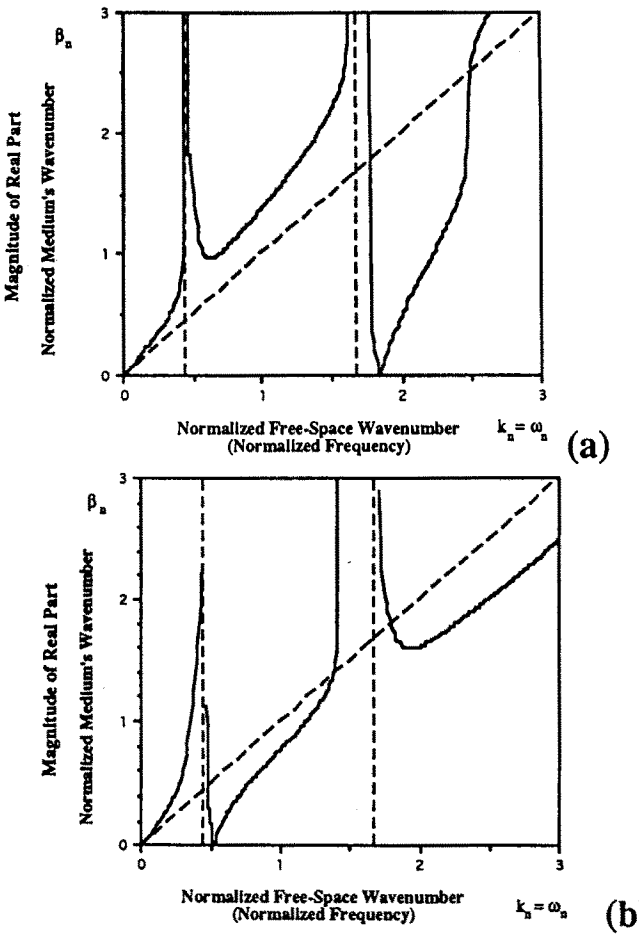

Figure 12. The vertical axes represent the magnitude (with no sign accounted) of the real part of normalized wavenumbers of a non–local Ω medium with (a) positive coupling admittance, and (b) negative coupling admittance. The medium specifications are the same as for Fig. 10, except that $l = 0.25\lambda_{co}$. Note that the first resonance frequency occurs at a lower frequency than the natural resonance frequency of the local Ω elements. [Remark: these plots were actually calculated assuming very small loss tangent of the host dielectric $\left(\delta = 10^{-6}\right)$. Including a small imaginary part into the permittivity, improves the convergence of the numerical solution of (35) by Newton's method. The curves shown are, therefore, the magnitude of the real part of the propagation constant. We made sure that the imaginary part corresponding to these curves (which is very small, of the order 10^7) is positive for all frequencies. It must also be mentioned that the numerical accuracy near resonance is much lower than that at a frequency far from it.]

at the graphs of effective permittivity and permeability of a non–local Ω medium, like those given in Fig. 9, we find that both parameters increase to infinitely large values for frequencies just below the resonance frequencies of the medium, and that they drop to infinitely negative values for frequencies just beyond these same frequencies. The same figure also shows that the product of permeability times coupling admittance reverses sign each time a resonance frequency is crossed, this product being infinitely large for frequencies in the neighborhood of the resonance frequencies. Equation (13) also shows that a positive coupling admittance has a tendency to reduce the propagation constant, while a negative Ω_c has a tendency to increase it.[7] Compiling this information allows us to arrive at the following explanation of the dispersion diagram for the non–local Ω medium.

(1) For frequencies between zero and the first resonance frequency, the value of effective permittivity and permeability is so high that it offsets any effect of the coupling admittance. Therefore, irrespective of the sign of the coupling admittance, the propagation constant of the medium increases monotonically from zero to an infinitely large value for frequencies just below the first resonance frequency.

(2) Beyond the first resonance, the coupling admittance reverses sign. Therefore, a medium whose coupling admittance is positive at low frequency changes into one with negative Ω_c. As a negative coupling admittance tends to increase the propagation constant, the drop in the effective permittivity and permeability that takes place for frequencies above resonance and near the cutoff band, is partially compensated for by the negative coupling admittance. The net result is that the propagation constant of a non–local medium, with positive low–frequency coupling admittance, does *not* drop to a very low value beyond the first resonance frequency. As the frequency is further increased, the conditions of the second resonance are approached and the effective permittivity and permeability rise again. Consequently, the (magnitude (absolute value) of real part of) propagation constant continues to increase to very large values for frequencies just below the second resonance. As the second resonance is passed, the coupling admittance changes its sign back to positive. For frequencies above the second reso-

[7] Although (13) was derived for infinitesimal Ω_c, its application here is justified due to the fact that the term in (35) that is linear in Ω_c, has only a single pole at resonance while the term involving the product $(\mu_{xx}\varepsilon_{yy})$ has a double pole at the same frequency.

nance frequency and near the second cutoff band, the effective permittivity and permeability are small in magnitude, and at the same time the coupling admittance is positive. All these conditions combine to reduce the value of the propagation constant to a very low value. As the frequency is increased and the conditions of the third resonance are approached, the propagation constant starts to increase gradually. From the above analysis (for the approximate circuit model), we conclude that the cutoff bands of a non–local Ω medium, whose low–frequency coupling admittance is positive, appear to be wider following the *even* resonance frequencies (i.e. the second, fourth, etc.) than it is for the odd ones.

(3) The situation for a medium whose low–frequency coupling admittance is negative is the opposite of the above described case. In particular, the (magnitude (absolute value) of real part of) propagation constant for the medium shown in Fig. 12b, is lower for the non–local Ω medium than it is for the host dielectric for almost the entire frequency range between the first and second resonance frequencies. If the properties of the non–local Ω medium are sought for the purpose of reducing guided surface waves, then this coupling admittance sign and frequency range constitute the appropriate choices. Note that this coupling admittance sign is achieved by *twisting* the loops of the non–local Ω elements 180° about the medium axis.

Apart from the phenomenon of resonance, the frequency characteristics of the propagation constant of the non–local Ω medium, as deduced from our simplistic approximate circuit model, are generally well behaved. The propagation constant is a single–valued continuous function of frequency between the resonance frequencies.[8] Based on this model, all values of propagation constant are allowable and there are no wavenumber band gaps.

In the next sub-section, we treat the problem of uniform plane wave propagation, in an arbitrary direction in an unbounded non–local pseudo–chiral Ω medium.

(b) *Propagation in a Three Dimensional Non-Local Ω Medium*

The vector algebraic equation governing the electric field of a

[8] Of course, since (35) is an even expression in terms of β, mathematically speaking, β can be either positive or negative. Here in Fig. 12, the magnitude (i.e., absolute value) of the real part of β is plotted.

uniform plane wave propagating in an arbitrary direction of a three-dimensional non-local Ω medium is given by (10). This equation can be rewritten in matrix form as $\mathbf{AE}_0 = 0$ where the vector $\mathbf{E}_0$ and the matrix $\mathbf{A}$ are given by,

$$\mathbf{E}_0 = \begin{bmatrix} E_{ox} \\ E_{oy} \\ E_{oz} \end{bmatrix} \tag{36a}$$

$$A = \begin{bmatrix} \omega^2\varepsilon_{xx} - \frac{k_y^2}{\mu_{zz}} - \frac{k_z^2}{\mu_{yy}} & \frac{k_x k_y}{\mu_{zz}} & \frac{k_x k_z}{\mu_{yy}} \\ \frac{k_y k_x}{\mu_{zz}} & \omega^2\varepsilon_{yy} - \frac{k_x^2}{\mu_{zz}} - \frac{k_z^2}{\mu_{xx}} - 2\omega\Omega_c k_z \sin(k_z l) & \frac{k_y k_z}{\mu_{xx}} - \mathrm{i}\omega\Omega_c k_y \mathrm{e}^{\mathrm{i}k_z l} \\ \frac{k_z k_x}{\mu_{yy}} & \frac{k_z k_y}{\mu_{xx}} + \mathrm{i}\omega\Omega_c k_y \mathrm{e}^{-\mathrm{i}k_z l} & \omega^2\varepsilon_{zz} - \frac{k_x^2}{\mu_{yy}} - \frac{k_y^2}{\mu_{xx}} \end{bmatrix} \tag{36b}$$

Equation (36) has a non-trivial solution if and only if the determinant of the matrix $\mathbf{A}$ vanishes. Equating the determinant of the matrix $\mathbf{A}$ to zero, we get the following equation;

$$\begin{aligned} k_0^2 \Bigg\{ & \frac{\varepsilon_{r_{xx}} k_x^4}{\mu_{r_{yy}}\mu_{r_{zz}}} + \frac{\left(\varepsilon_{r_{yy}} + \mu_{r_{xx}}\alpha_c^2\right) k_y^4}{\mu_{r_{zz}}\mu_{r_{xx}}} + \frac{\varepsilon_{r_{zz}} k_z^4}{\mu_{r_{xx}}\mu_{r_{yy}}} + \left(\frac{\varepsilon_{r_{xx}}}{\mu_{r_{xx}}} + \frac{\varepsilon_{r_{yy}}}{\mu_{r_{yy}}}\right)\frac{k_x^2 k_y^2}{\mu_{r_{zz}}} \\ & + \left(\frac{\varepsilon_{r_{yy}} + \mu_{r_{xx}}\alpha_c^2}{\mu_{r_{yy}}} + \frac{\varepsilon_{r_{zz}}}{\mu_{r_{zz}}}\right)\frac{k_y^2 k_z^2}{\mu_{r_{xx}}} + \left(\frac{\varepsilon_{r_{zz}}}{\mu_{r_{zz}}} + \frac{\varepsilon_{r_{xx}}}{\mu_{r_{xx}}}\right)\frac{k_z^2 k_x^2}{\mu_{r_{yy}}} \\ & - \varepsilon_{r_{xx}}\left(\frac{\varepsilon_{r_{yy}}}{\mu_{r_{yy}}} + \frac{\varepsilon_{r_{zz}}}{\mu_{r_{zz}}}\right) k_x^2 k_0^2 - \left(\frac{\varepsilon_{r_{yy}}\varepsilon_{r_{zz}}}{\mu_{r_{zz}}} + \frac{\varepsilon_{r_{xx}}\left(\varepsilon_{r_{yy}} + \mu_{r_{xx}}\alpha_c^2\right)}{\mu_{r_{xx}}}\right) k_y^2 k_0^2 \\ & - \varepsilon_{r_{zz}}\left(\frac{\varepsilon_{r_{xx}}}{\mu_{r_{xx}}} + \frac{\varepsilon_{r_{yy}}}{\mu_{r_{yy}}}\right) k_z^2 k_0^2 + \varepsilon_{r_{xx}}\varepsilon_{r_{yy}}\varepsilon_{r_{zz}} k_0^4 \\ & + 2\alpha_c k_0 k_z \sin(k_z l)\left[\frac{\varepsilon_{r_{xx}} k_x^2}{\mu_{r_{yy}}} + \frac{\varepsilon_{r_{zz}} k_y^2}{\mu_{r_{zz}}} + \frac{\varepsilon_{r_{zz}} k_z^2}{\mu_{r_{yy}}} - \varepsilon_{r_{xx}}\varepsilon_{r_{zz}} k_0^2\right] k_z^2 \Bigg\} = 0 \end{aligned} \tag{37}$$

where subscript r denotes relative quantities with respect to corresponding quantities of free space. Equation (37) is a fourth–order equation in the unknowns k_x, k_y and k_z. For a given frequency ω, or equivalently, for a given free–space propagation constant k_0, this equation represents a double–folded closed surface in the k–space. This surface is known as the *normal surface* [14]. This surface is also known as the *index surface,* since it contains all the information required to determine the medium's index of refraction along any direction [15]. The medium's index of refraction, which is equal to the ratio of the propagation constant in the medium to that in free-space, can be determined from the index surface in the following way. A ray is projected from the origin, pointing in the specific direction, along which it is required to find the index of refraction. In general, the ray intersects with the index surface at two distinct points. The medium's propagation constant, along the direction of the ray, is determined by the length of the k–vectors connecting the origin to these intersection points. Therefore, in general, the medium has two different values for the propagation constant along any direction, and, consequently, two values for its index of refraction. By substituting the coordinates (k_x, k_y, k_z) of one or the other of the two intersection points into the matrix $\mathbf{A}$ and solving for $\mathbf{E}_0$, we obtain the polarization state of the eigenmode of propagation corresponding to our choice of wavenumber. This procedure is illustrated by an example below.

Consider for example, a wave propagating parallel to the $x-z$ plane. This is equivalent to saying that the k–vector lies in the k_x-k_z plane (i.e., $k_y = 0$ plane). In this case, (37) reduces to,

$$\begin{aligned}&\left(\varepsilon_{r_{xx}}k_x^2 + \varepsilon_{r_{zz}}k_z^2 - \varepsilon_{r_{xx}}\varepsilon_{r_{zz}}\mu_{r_{yy}}k_0^2\right)\\ &\cdot\left(\mu_{r_{xx}}k_x^2 + \mu_{r_{zz}}k_z^2 - \mu_{r_{xx}}\mu_{r_{zz}}\varepsilon_{r_{yy}}k_0^2 + 2\alpha_c\mu_{r_{xx}}\mu_{r_{zz}}k_0k_z\sin(k_zl)\right) = 0\end{aligned} \tag{38}$$

Each factor on the left–hand–side of this equation, can be individually made equal to zero, giving rise to the equation of one or the other of the intersection curves of the index surface with the $k_y = 0$ plane. These curves are shown in Fig. 13 for a typical non–local Ω medium. The figure also shows the polarization states of the different eigenmodes. If θ is the angle between the ray $\vec{OR}$ and the z axis, then the components of the k–vector of a wave propagating parallel to the $x-z$ plane can be written as, $k_x = k\sin(\theta)$, $k_y = 0, k_z = k\cos(\theta)$. Equating the first factor on the left–hand side of (38) to zero and substituting for k_x and k_z from the above relation, we get the following expression for

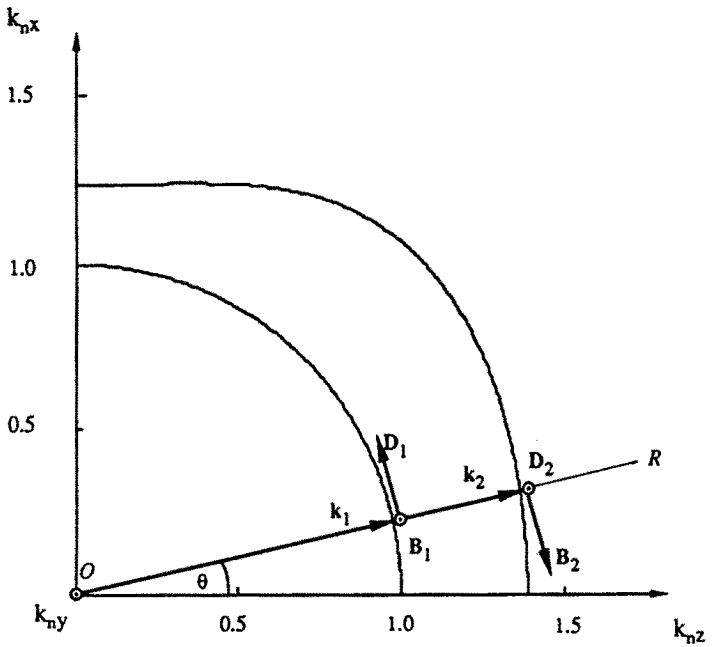

Figure 13. This figure shows the intersection of the index surface with the $k_y = 0$ plane. Only the first quadrant is shown since (37) has even symmetry with respect to all of the three principal planes. The medium parameters are the same as for Fig. 12a. The operating frequency is $k_o = k_{co}$, the resonance frequency of the local Ω elements. The two possible wavenumbers for a wave propagating along the direction of the ray $\vec{OR}$, are given by the length of the vectors k_1 and k_2. The eigenmodes corresponding to these wavenumbers are also shown symbolically by displaying their polarization.

$$k_1(\theta) = \frac{\sqrt{\varepsilon_{r_{xx}}\varepsilon_{r_{zz}}\mu_{r_{yy}}}k_0}{\sqrt{\varepsilon_{r_{xx}}\sin^2(\theta) + \varepsilon_{r_{zz}}\cos^2(\theta)}} \tag{39}$$

The eigenmode corresponding to this wavenumber has its magnetic field polarized along the y-axis and its electric field parallel to the $x - z$ plane. If we take the z-direction to be the "preferred" direc-

$$k_1(\theta) = \frac{\sqrt{\varepsilon_{r_{xx}}\varepsilon_{r_{zz}}\mu_{r_{yy}}}k_0}{\sqrt{\varepsilon_{r_{xx}}\sin^2(\theta) + \varepsilon_{r_{zz}}\cos^2(\theta)}} \tag{39}$$

The eigenmode corresponding to this wavenumber has its magnetic field polarized along the y-axis and its electric field parallel to the $x-z$ plane. If we take the z-direction to be the "preferred" direction of propagation, then we can classify this eigenmode as a TM wave. Considering the orientation of the Ω elements in the medium, which is shown in Fig. 4, it is clear that a field having this polarization does *not* interact with these Ω elements. Therefore, this eigenmode is identical to the corresponding one in the host dielectric. Equating the second factor on the left-hand side of (38) to zero and performing the substitutions for k_x and k_z, we find that the magnitude of the propagation constant of the second mode is obtained by *solving* the following equation,

$$\begin{aligned}&\left(\mu_{r_{xx}}\sin^2(\theta) + \mu_{r_{zz}}\cos^2(\theta)\right)k_2^2(\theta)\\ &+ 2\alpha_c\mu_{r_{xx}}\mu_{r_{zz}}\cos(\theta)k_0k_2(\theta)\sin\left(k_2(\theta)l\cos(\theta)\right)\\ &- \mu_{r_{xx}}\mu_{r_{zz}}\varepsilon_{r_{yy}}k_0^2 = 0\end{aligned} \tag{40}$$

This eigenmode has its electric field polarized along the y-axis and its magnetic field parallel to the $x-z$ plane. Using the above mentioned terminology, this wave can be classified as a TE wave. A field having this polarization interacts strongly with the Ω elements in the medium. In the case of a non-local Ω medium, the effect on wavenumber is proportional to the first order of magnitude of the coupling admittance.

As far as the wave characteristics are concerned, the second eigenmode, i.e., the TE wave which interacts with the Ω elements, does not essentially differ much from the linearly polarized eigenmodes of propagation in ordinary anisotropic (e.g., dielectric) media. The only difficulty associated with the Ω-medium eigenmode is that its wavenumber cannot be obtained in a closed form formula. Instead, it has to be obtained by solving a transcendental algebraic equation, viz. (40). Unlike the case of ordinary anisotropic media, where the eigenmodes are obtained by means of the *index ellipsoid,* it appears that there is no obvious way to obtain the eigenmodes in the bi-anisotropic Ω medium. Figures 14 show the intersection of the index surface with the three principal planes in the k-space. Only the first octant is shown, since (37) has even symmetry with respect to all of the three principal

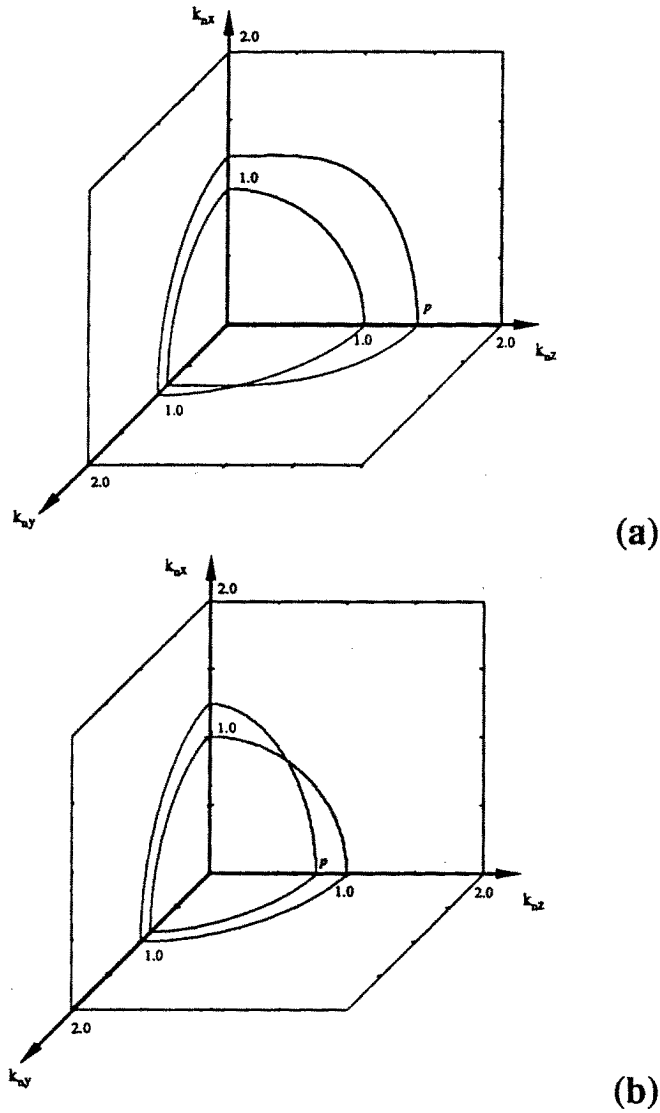

Figure 14. This figure shows the intersection of the index surface of a non–local Ω medium, with (a) positive Ω_c and (b) negative Ω_c, with the three principal planes in the k–space. The medium and operating frequency are the same as for Fig. 13. Compare the position of the point p on part (a) to its position on part (b). This point indicates the intersection of the z–axis with the index-surface-fold that belongs to the strongly affected eigenmode.

k–planes.[9] Both positive and negative coupling admittance are considered. The effect of the coupling admittance sign on the propagation along the medium's translational axis, i.e. the z–axis, is obvious. Propagation transverse to the medium's axis is not affected by the sign of Ω_c. We conclude this sub–section on plane wave propagation by listing the polarization states of the eigenmodes of propagation along the principal axes. Whenever possible, we also provide the explicit value of the propagation constant and the wave impedance. Otherwise, we provide the equation governing the wavenumber.

(1) *Propagation along the x–axis:*

First eigenmode: a TEM wave:

The electric field is polarized along the z–axis, $E_{ox} = 0$, $E_{oy} = 0$, $E_{oz} = E_0$. The propagation constant is given by $\beta = \sqrt{\varepsilon_{r_{zz}}\mu_{r_{yy}}}k_0$. The wave impedance is given by $\eta = \sqrt{\frac{\mu_{r_{yy}}}{\varepsilon_{r_{zz}}}}\eta_0$.

Second eigenmode: a TE wave:

The electric field is polarized along the y–axis. $E_{ox} = 0$, $E_{oy} = E_0$, $E_{oz} = 0$. The propagation constant is given by $\beta = \sqrt{\varepsilon_{r_{yy}}\mu_{r_{zz}}}k_0$. The wave impedance (as defined by $-E_y/H_z$) is given by $\eta = \sqrt{\frac{\mu_{r_{zz}}}{\varepsilon_{r_{yy}}}}\eta_0$. The analogy of this eigenmode to the TE plane waves in transversely biased ferrites constitute the basis for the design of rectangular-waveguide slab phase shifters reported in [1].

(2) *Propagation along the y-axis:*

First eigenmode: a TEM wave:

The electric field is polarized along the x–axis, $E_{ox} = E_0$, $E_{oy} = 0$, $E_{oz} = 0$. The propagation constant is given by $\beta = \sqrt{\varepsilon_{r_{xx}}\mu_{r_{zz}}}k_0$. The wave impedance is given by $\eta = \sqrt{\frac{\mu_{r_{zz}}}{\varepsilon_{r_{xx}}}}\eta_0$.

---

[9] Incidentally, this means that replacing k by $-k$ leaves (3.5.6) invariant. Consequently, the propagation constant does not depend on the sense of propagation, as seen in reciprocal media.

Second eigenmode: a TM wave:

The electric field is polarized along the z-axis with a non-vanishing longitudinal component. $E_{ox} = 0$, $E_{oy} = \dfrac{\mathrm{i}\alpha_c\sqrt{\varepsilon_{r_{zz}}\mu_{r_{xx}}}}{\sqrt{\varepsilon_{r_{yy}}\left(\varepsilon_{r_{yy}} + \mu_{r_{xx}}\alpha_c^2\right)}}E_0$, $E_{oz} = E_0$ where the effect of the Ω-transmission lines are taken into ε_{zz}. The propagation constant is given by

$$\beta = \sqrt{\varepsilon_{r_{zz}}\mu_{r_{xx}}}\cdot\sqrt{1 - \frac{\mu_{r_{xx}}\alpha_c^2}{\varepsilon_{r_{yy}} + \mu_{r_{xx}}\alpha_c^2}}k_0.$$

The wave impedance is given by

$$\eta = \frac{\eta_0}{\dfrac{\beta}{\mu_{r_{xx}}k_0} - \dfrac{\alpha_c^2\exp(-\mathrm{i}\beta l)\sqrt{\varepsilon_{r_{zz}}\mu_{r_{xx}}}}{\sqrt{\varepsilon_{r_{yy}}\left(\varepsilon_{r_{yy}} + \mu_{r_{xx}}\alpha_c^2\right)}}}.$$

(3) *Propagation along the z-Axis:*

First eigenmode: a TEM wave:

The electric field is polarized along the x-axis. $E_{ox} = E_0$, $E_{oy} = 0$, $E_{oz} = 0$. The propagation constant β is given by $\beta = \sqrt{\varepsilon_{r_{xx}}\mu_{r_{yy}}}k_0$. The wave impedance η is given by $\eta = \sqrt{\dfrac{\mu_{r_{yy}}}{\varepsilon_{r_{xx}}}}\eta_0$.

Second eigenmode: a TEM wave:

The electric field is polarized along the y-axis. $E_{ox} = 0$, $E_{oy} = E_0$, $E_{oz} = 0$. The propagation constant is a solution of the following equation $\beta^2 + 2\alpha_c\mu_{r_{xx}}k_0\beta\sin(\beta l) - \mu_{r_{xx}}\varepsilon_{r_{yy}}k_0^2 = 0$. The wave impedance is given by

$$\eta = \frac{\eta_0}{\dfrac{\beta}{\mu_{r_{xx}}k_0} + \mathrm{i}\alpha_c\exp(-\mathrm{i}\beta l)},$$

$$|\eta| = \frac{\eta_0}{\sqrt{\left(\dfrac{\beta}{\mu_{r_{xx}}k_0} + \alpha_c\sin(\beta l)\right)^2 + \alpha_c^2\cos^2(\beta l)}}$$

Note that both of the wavenumber and the wave impedance of this eigenmode depend to the first order on the coupling admittance Ω_c.

7. Summary

In this paper, we introduced and discussed the concept of the non–local Ω medium as a generalization to the local Ω medium, introduced originally in our previous work [1]. The medium can, in principle, be constructed by embedding a large number of non–local Ω elements in an isotropic host dielectric. The non–local Ω medium was conceived in an attempt to find an example of bianisotropic media with Ω elements that strongly interact with linearly polarized TEM uniform plane waves. The conditions under which it can be justified to describe such a medium, by a set of constitutive relations, are also discussed. It is claimed that if the field propagates mainly in the direction of the translational symmetry of the non–local Ω medium, and, particularly, if its electric field is polarized normal to the Ω–transmission lines (as it is the case for a TE wave), then the medium can be described by a set of constitutive relations. The constitutive relations of the non–local Ω medium were presented and discussed. It was shown that performing a Fourier transform with respect to the spatial variable, along the direction of the medium's translational symmetry axis, reduces the form of the constitutive relations to that of a local medium. The electric–field wave equation was presented and also subjected to the same simplifying transform. By its nature, the non–local Ω medium is a dispersive medium. Therefore, it was necessary that we consider the frequency characteristics of its material parameters. For this purpose, we suggested a lumped–element simplistic equivalent circuit of the non–local Ω element and used it to calculate the induced electric and magnetic dipole moment densities in the medium. The frequency characteristics of the local and non–local Ω media were presented and commented upon. The model, which is valid for low and intermediate frequencies, exhibits many features and provides, in general, physically acceptable results. The model fails to predict the high frequency limit of the medium's permeability. However, as described in the text, this is a result of the approximations that are inherent in modeling the Ω element by lumped–element equivalent circuit. The propagation of uniform plane waves in a non–local Ω medium was also studied. The propagation along the medium's symmetry axis was studied and the propagation constant, as a function of frequency, given. The results showed the first order effect of the coupling admittance on the wavenumber. The propagation in an arbitrary direction in a

three-dimensional Ω medium was studied and the wavenumber given in terms of the index surface. Finally, the eigenmodes of propagation and the wave impedance were given for wave propagation along the principal coordinate axes.

Acknowledgments

This work was supported, in part, by the U.S. National Science Foundation under Presidential Young Investigator Grant No. ECS-8957434.

References

1. Saadoun, M. M. I., and N. Engheta, "A reciprocal phase shifter using novel pseudochiral Ω medium", *Microwave and Opt. Tech. Lett.,* Vol. 5, No. 4, 184–188, 1992.
2. Engheta, N., and M. M. I. Saadoun, "Novel pseudochiral or Ω medium and its applications," Abstract in *Proceedings of Progress in Electromagnetic Research Symposium (PIERS'91),* Cambridge, MA, 339, July 1991.
3. Saadoun, M. M. I., and N. Engheta, "Novel designs for reciprocal phase shifters using pseudochiral or Ω medium," Abstract in *Digest of the 1991 IEEE AP-S/URSI Symposium,* London, Ontario, Canada, Vol. URSI Digest, 337, June 1991.
4. Saadoun, M. M. I., and N. Engheta, *"The pseudochiral Ω medium: What is it? And what can it be used for?," Digest of the 1992 IEEE AP-S/URSI Joint Symposia,* Chicago, Illinois, Vol. AP-4, 2038–2041, July 1992.
5. Kong, J. A., *Theory of Electromagnetic Waves,* Wiley Interscience, New York, 1975.
6. Kong, J. A., "Theorems of bianisotropic media", *Proc. IEEE,* Vol. 60, No. 9, 1036–1046, Sept. 1972.
7. Saadoun, M. M. I., "The pseudochiral omega (Ω) medium: theory and potential applications," Ph.D. Dissertation, Department of Electrical Engineering, University of Pennsylvania, October 1992.
8. Saadoun, M. M. I., and N. Engheta, "Pseudochiral Ω medium and guided–wave structures: theory and principles," *Proceedings of the 14th Triennial URSI International Symposium on Electromagnetic Theory,* Sydney, Australia, 302–304, August 1992.

9. Sihvola, A., and I. V. Lindell, "Chiral Maxwell–Garnett mixing formula," *Electr. Lett.,* Vol. 26, No. 2, 118–119, 1990.
10. Brillouin, N., *Wave Propagation in Periodic Structures,* McGraw Hill, New York, 1946.
11. Brillouin, L., *Wave Propagation and Group Velocity,* Academic, New York, 1960.
12. Emeis, C. A., and L. J. Osterhoff, G. De Vries, "Numerical evaluation of Kramers–Kronig relations", *Proc. Roy. Soc. Lond. A.,* Vol. 297, No. 1, 54–65, 1967.
13. Engheta, N. and P. Zablocky, "A step towards determining transient response of chiral materials: Kramers-Kronig relations for chiral parameters", *Electr. Lett.,* Vol. 26, No. 25, 2132–2134, 1990.
14. Yariv, A. and P. Yeh, *Optical Waves in Crystals,* John Wiley & Sons, New York, 1984.
15. Born, M. and E. Wolf, *Principles of Optics,* Pergamon Press, New York, 1980.
16. Tretyakov, S. A., "Thin pseudochiral layers– approximate boundary conditions and potential applications," *Microwave and Opt. Tech. Lett.,* Vol. 6, No. 2, 112–115, 1993.
17. Lindell, I. V., S. A. Tretyakov, and A. J. Viitanen, "Plane–wave propagation in a uniaxial chiro–omega medium," *Microwave and Opt. Tech. Lett.,* Vol. 6, No. 9, 517–520, 1993.
18. Schelkunoff, S. A., and H. T. Friis, *Antenna Theory and Practice,* John Wiley & Sons, New York, 1952.